Ultrasound

J. Cornwall, Chair
H. Abarbanel
W. Dally
S. Flatté
R. Westervelt

May 1996

JSR-95-145

REPORT DOCUMENTATION PAGE

1. AGENCY USE ONLY (Leave blank)	2. REPORT DATE May 1996	3. REPORT TYPE AND DATES COVERED

4. TITLE AND SUBTITLE

ULTRASOUND

6. AUTHOR(S)

H. Abarbanel, J. Cornwall, W. Dally, S. Flatte, R. Westervelt

5. FUNDING NUMBERS

07-95-8534-A4

7. PERFORMING ORGANIZATION NAME(S) AND ADDRESS(ES)

The MITRE Corporation
JASON Program Office, Z561
1820 Dolley Madison Blvd
McLean, Virginia 22102

8. PERFORMING ORGANIZATION REPORT NUMBER

JSR-95-145

9. SPONSORING/MONITORING AGENCY NAME(S) AND ADDRESS(ES)

DARPA/TIO
3701 North Fairfax Drive, Arlington, Va 22030-1714

10. SPONSORING/MONITORING AGENCY REPORT NUMBER

JSR-95-145

11. SUPPLEMENTARY NOTES

12a. DISTRIBUTION/AVAILABILITY STATEMENT

Approved for Public Release. Distribution Unlimited

12b. DISTRIBUTION CODE

Limiter Statement A

13. ABSTRACT (Maximum 200 words)

This report deals with the technical issues in ultrasound, both for combat and civilian care, which are most likely to benefit from support from an agency like DARPA which is responsive to long-horizon problems requiring innovative technology.

14. SUBJECT TERMS

15. NUMBER OF PAGES

16. PRICE CODE

17. SECURITY CLASSIFICATION OF REPORT	18. SECURITY CLASSIFICATION OF THIS PAGE	19. SECURITY CLASSIFICATION OF ABSTRACT	20. LIMITATION OF ABSTRACT
Unclassified	Unclassified	Unclassified	SAR

Contents

1 EXECUTIVE SUMMARY

1.1 Introduction

In the summer of 1995 JASON conducted its third study on the ARPA biomedical technology program. This study was devoted to ultrasound, following ARPA's decision last year to fund ultrasound research for combat casualty care at a level up to $35M over a period of five years. Proposals for these funds are due in September 1995, following the close of the summer study, and we neither saw nor judged the merits of any proposal to ARPA. Instead, we dealt with the technical issues in ultrasound, both for combat and civilian care, which are most likely to benefit from support from an agency like ARPA which is responsive to long-horizon problems requiring innovative technology.

ARPA's Broad Agency Announcement (BAA) contains the following language:

> ARPA seeks proposals to develop the technology of medical ultra-
> sonic imaging for improved diagnostic utility in forward echelon
> combat care... The primary technical target for this program is
> improvement in diagnostic utility of ultrasound images obtained
> by correcting for aberration in the propagation of the ultrasound
> beam in tissue. Technical issues to be addressed include one-and-
> a-half or two dimensional transducer array technology, electronics

for real-time adaptive beam forming, signal processing to eliminate false targets, and the appropriate image display electronics. Additional technical targets encompass three dimensional imaging and compact, low-power, portable imagers... For field portable imagers, a technical issue, beyond the transducer, electronics, and display, is an appropriate telemetry interface to allow rear echelon participation in diagnosis... To the extent that a compelling case can be made for significant technical opportunities linked to important defense needs, alternate technical targets in medical ultrasonic technology development may be included in the program.

It will be seen that the BAA addresses, among other things, two of the important technology objectives identified in our earlier reports: means for adaptive image correction and the design and construction of two-dimensional (2D) arrays. Our report concentrates on these two issues, which are related in more than one way.

Below we give an overview of the major issues (covered in greater depth in the main body of the report), and then our conclusions and recommendations.

1.2 The Ultrasound Community and Other Technology Communities

The ultrasound community concerned with technology has two components, university (and other nonprofit) researchers, and commercial companies. There is some, but not much, componentry development in the university community. Ultrasound manufacturers often have connections with university research groups which are allowed to use new commercial developments before they reach the market. The commercial sector develops products on the basis of near-term marketability and keeps quiet about its long-term in-house research efforts (about which we know little). The result is that there are few non-commercial efforts to develop components, to work on long-horizon projects, or projects with some risk, either technically or in potential marketability. Nor is there much impetus from the traditional ultrasound funding agencies (NIH, NSF) to move in these directions. Many very good researchers in ultrasound are eager to move in new and possibly quite productive areas of ultrasound research, but little funding is available for advanced technology development, and sophisticated fabrication facilities are not available to university researchers. A number of other technologies may have much to contribute to ultrasound, but the workers in these areas are not familiar with the detailed problems of ultrasound. Most, if not all, of these technologies have been supported by ARPA; they include MEMS (microelectromechanical systems), imaging sonar, advanced processing, image understanding, and knowledge-based systems. ARPA can play a major role in bringing about the appropriate technology merger. In many cases,

3

this will call for teaming of these other ARPA research communities with the ultrasound workers, since neither side is necessarily familiar with the difficulties and opportunities of the other. But in some cases this gap may impede the communication needed to form good teams and ARPA may find it more valuable to let various technologies evolve independently provided that there is a reasonably clear path toward an ultimate merger benefitting ultrasound.

1.3   Forward Echelon Medical Care

The use of ultrasound in forward echelon medical care is not just a matter of trundling out a commercial machine. Several novel developments are needed, which will assist not only in civilian trauma care but will have other influences as well in traditional ultrasound arenas. Battlefield ultrasound images may require immediate interpretation by people who are not trained radiologists, perhaps medical corpsmen who must make decisions for emergency care without consulting an MD, or at best a non-radiologist MD. Improvement in deaberration technology may well have its biggest impact for non-radiologist personnel. For combat medical care, these improvements must be coupled with enhancements in image understanding and knowledge-based interpreters, which among other things may use edge-finding algorithms, standard anatomic ultrasound maps for comparison purposes, automatic recognition of certain key diagnostic features for trauma, and the like.

There is a strong synergy between technology designed for aberration control and that designed for image understanding; for example, an original aberrated image may be interpreted by system software (not people) to yield outline maps of areas of different sound speeds, the speeds being assigned a priori by a knowledge-based system which understands the difference between fat, muscle, etc. These maps may then be used by the system to deaberrate large-scale refractive errors and the result used as input to a different deaberrator such as a time-delay compensator. Trauma care also lends itself to the application of certain deaberration schemes which might seem unattractive in a non-emergency context: contrast agents may be injected along with blood plasma or other medication and used as beacons for deaberration schemes like those used in astronomy. Such developments will have a major impact on civilian non-emergency ultrasound and will be useful to radiologists as well as other MDs.

Finally, it goes almost without saying that battlefield care will require development of small hand-portable ultrasound equipment as well as more sophisticated and possible larger units which incorporate more of the technology we discuss.

1.4 2D Transducers

Current commercial off-the-shelf (COTS) ultrasound transducer arrays have about 100 elements in a line, with poor resolution in the direction transverse to the array line. Commercial companies are planning so-called

1.5D arrays with about 1000 elements, in roughly 100×10 configuration, again with poor resolution in one direction (mostly because the pixels are long and thin, averaging over the long direction). These arrays use the same physical pixels for both receive and transmit. We believe that the major breakpoint for 2D arrays, either filled or sparse, is at a size of 100×100 with square pixels and equal resolution in both directions. Anything smaller is only an incremental improvement over planned commercial developments and will sacrifice resolution or sidelobes in one dimension.

It is not necessary to colocate the ultrasound receiver and transmitter or to use the same technology in both. In fact, there may be good reasons in deaberration to separate the two. For this and other reasons we believe it is worthwhile to investigate alternate technologies for receive arrays, not just conventional piezoelectric materials.

Large 2D arrays bring about numerous problems which we believe are soluble but which will require some advanced technology: there are many more connections, electronics power dissipated in the transducer gets large (at least with conventional equipment), and signal processing must be done at high rates. Partly for these reasons several researchers are working on large but unfilled arrays, with many more pixel positions on the array than there are active pixels. (Unfilled arrays improve resolution, but lead to increased sidelobes; the sidelobe problem is, however, manageable.) There are several ongoing ARPA-sponsored programs relevant here, notably on MEMS.

1.5 Deaberration

While deaberration is a very active field, it is an interesting comment on its maturity that no commercial ultrasound equipment uses true adaptive imaging. There are two major approaches which do not depend on in-tissue beacons: time-delay compensation schemes, which use forward or backscatter geometries, and inverse scattering or tomographic schemes dependent on gathering data along many lines of sight. The former are accurate in principle only if all the aberrators are very close to the receiver (but usably accurate if the phase aberrations are small or if the curvature of the wavefront is small) and the latter are likely to be impractical in real-world applications, at least at an attractive cost. (Some workers are developing methods, quite worthy of further investigation, based on limited angular diversity or redundancy of images. Such methods, when fully developed, may be a good compromise between single-aspect deaberration techniques and full inverse scattering.) There is evidence that the conditions for time-delay compensation are sometimes met in tissue, but lack of good 2D resolution degrades their utility.

Schemes using point targets in tissue are considered to be practical only in specialized circumstances, but if injected contrast agents are used (these consist of resonantly-scattering point targets) such deaberration ideas may become useful. In battlefield care contrast agents can be introduced along with blood plasma or other medication. A 2D transmit array with sufficient resolution could be used to focus the ultrasound beam on a bright reflector, such as bone. One idea which uses one or more bright point-like targets in the

tissue medium is of particular interest: time reversal allows one to focus an ultrasound beam on such targets, and may be useful in defining propagation corrections for sound paths passing near the targets.

The old idea of compound scanning, or incoherent fusion of images taken from several aspects, has seen a limited revival in forming high-quality limb images for use in prosthesis manufacture. Deaberration with more sophisticated algorithms may also require compound images, taken with separate receivers and transmitters.

There are several areas in deaberration which deserve more attention. Little is being done about trying to deaberrate relatively large-scale (compared to a wavelength) smooth variations in sound speed in a deterministic way, that is, by understanding the tissue medium's specific properties on such spatial scales. At these scales it makes sense to make a preliminary image at low frequencies (0.5-1 MHz) which suffers far less from attenuation and has more relaxed processing requirements. There are few basic theoretical studies of the quantitative improvement in image quality that various deaberration techniques will produce, given a characterization of the aberrating medium; instead, there are many simulations and experiments, both in tissue and in phantoms (ultrasound targets of known aberration characteristics). Little is known about how deaberration schemes intermediate between forward or backscatter geometry and full inverse scattering would work in practice. Not enough work is being done on comparisons of different deaberration techniques on the same target (tissue or phantom). It is important to note that adaptive acoustics for ultrasound is not a problem whose solution can be

carried over intact from other problems of propagation in aberrated media, such as the atmosphere, ocean, or solid earth. The ultrasound tissue medium is strongly attenuating (more so at higher frequency), has strong reflectors and refractors, and requires its own special investigation.

1.6 Tissue Characterization

In ultrasound, much of the tissue characterization work is done with the same instruments used to make images, with their (usual) limitation to backscatter operation. It has proven difficult to make crucial measurements such as attenuation constants of tissues, frequency dependence of the speed of sound in tissue, elastic constants, and the like by such means with high accuracy. In any case, tissue is variable from patient to patient and from one organ to another. Tissue characterization which attempts to aid clinical diagnosis by absolute measurements of properties has not proven useful, but measurements contrasting tissue types in the same overall tissue sample could be quite helpful; these include looking for differences between collagen and muscle in the heart, as an example. A program of tissue characterization would include sonoelasticity studies, mode conversion studies, investigations at multiple scattering angles, and other studies which go beyond the capability of conventional ultrasound equipment. It is not clear to us whether tissue characterization is more useful as an input to deaberration or in diagnosis.

This brief introduction should help to understand the following conclusions and recommendations. Supporting technical detail is contained in the body of the report.

1.7 Conclusions and Recommendations

1. The (non-commercial) ultrasound community is not developing the technology it needs to generate significant advances in ultrasound medical imaging, in part because its traditional funding sources do not support technology development to a great extent. Many current programs in ultrasound development are not sufficiently far-reaching and ambitious, perhaps in part because the radiology community is not aware of the possibilities for improvement that we discuss here. These improvements, if brought to fruition, will benefit not only trained radiologists but to an even greater extent non-radiologists who will be involved in forward echelon combat care. Several current ARPA programs are developing technology of high interest to future ultrasound enhancement, but the research communities in these technologies are not familiar with ultrasound.

WE RECOMMEND:

ARPA should take the opportunity to become the focus for both advanced software and hardware development in ultrasound, looking for sophisticated and possibly long-lead-time projects using MEMS, advanced processing hardware and software, on-array electronics, imag-

ing sonar, and the like which may otherwise not be developed for ultrasound. There is little to be gained by ARPA's funding of ultrasound programs outside of such areas of advanced technology or in providing augmentation of funds for current ultrasound projects if those projects are likely to yield only incremental technology improvements.

ARPA should look for ways to involve its image-understanding programs with ultrasound technology, so that even conventional ultrasound images (that is, without deaberration) can be better used by non-radiological medical personnel, especially in the context of battlefield care.

If the proposals received as a result of the BAA do not accord with the above recommendations, ARPA should issue detailed guidance to proposers which is designed to assist in bringing about the desired mergers of new and traditional technologies.

2. Deaberration of medical ultrasound images is not yet a quantitatively-understood subject, nor one which has made enough progress to warrant its incorporation in commercial equipment. Much current deaberration research is done with commercial off-the-shelf (COTS) equipment, which sharply narrows the horizons of the subject. There is little or no intercomparison of different deaberration schemes used on the same tissue sample or phantom. There is little work on adaptive acoustics schemes using in-tissue beacons. Deaberration theory tends to be limited to full inverse scattering or tomography, and needs developments specific to medical ultrasound and its tissue medium.

WE RECOMMEND:

ARPA should seek to fund a deaberration program going beyond incremental changes to COTS equipment. The elements of such a program might include:

- Incorporation of image-understanding techniques to generate a low-resolution map of the imaged tissue, assigning appropriate sound velocities to different tissues for use as part of a deaberration scheme to control gross refractive and reflective aberrations.

- Separated transmit and receive transducers for gathering data at several angles. Developments should be sought ranging from a revival of compound scattering to more sophisticated deaberration schemes using phase and amplitude information.

- Consideration of beacon-based schemes, including variants of time reversal. Beacons may be generated by injected contrast agents (air-filled microspheres) or by confocal illumination of natural reflectors in the body.

- A broad program in ultrasound deaberration theory, which will necessarily differ significantly from other theories of propagation in distorted media (e.g., the ocean, atmosphere, or earth) because of the specific nature of the tissue medium being imaged.

- Accompanying the theory program, simulations of the scattering physics with realistic tissue models (that is, computer generation of aberrated images) as test beds for arrays and deaberration.

— A protocol for standardization and benchmarking of deaberration experiments, as well as of theory and simulations.

3. 2D transducers are the holy grail of medical ultrasound technology, but current development plans of which we know fall short of what seems achievable in the next ten years. These planned arrays are too small (often because of what are thought of as nearly intractable interconnect problems), have pixel elements with poor resolution in one array direction, and are not matched with likely developments in microfabrication and on-array processing hardware. Generally the planned arrays are combined transmit/receive based on piezoelectric transducers. Much better arrays can be built within the next 5-10 years. Possible systems range from low data-rate confocal-scan systems to full 3D imaging in a single pulse, with a range of intermediate schemes. Data-handling rates can be very high, especially if advanced deaberration processing is necessary, and may lead to image production in less than real time. We believe that a delay of a few seconds or so is tolerable if the images are considerably better than they are now. 2D arrays may allow for automated search for the best image (as ultrasound technicians now search by hand). It appears that even in favorable tissue environments where simple time-delay deaberration works, 2D arrays are needed to resolve and correct the aberrations. Data-handling at the receiver and high-speed processing elsewhere are essential and doable.

WE RECOMMEND:

ARPA should set certain goals for the development of 2D transducers, including:

- Arrays should be at least 100×100, with square pixels, to get at least as good resolution in two dimensions as current linear arrays get in one, if the arrays are filled.

- For better axial resolution, development of even larger arrays should be started, beginning with sparse arrays and working toward large filled arrays. This will improve transverse resolution too, but for sparse arrays the sidelobe rejection will not be comparably improved.

- While integrated transmit/receive arrays will always be useful, a program of separate receive and transmit arrays should be developed, for many reasons, including use in better deaberration schemes and possible use of different techniques either for sending or receiving ultrasound. These techniques include capacitive microphone arrays, atomic-force microscope or similar sensor arrays, and fiber-optic technology.

- Development of on-transducer processing, including sample-and-hold electronics, multiplexers, and multiple low-power analog-to-digital converters to buffer the high data rates of large 2D arrays.

- Development of off-transducer processing power, both application-specific and COTS, for dealing with 2D signal processing and deaberration.

- Beam-forming techniques should be developed to allow automatic or joy-stick- guided taking of images from multiple aspects with a physically-fixed array.

14

1.8 Acknowledgements

2   INTRODUCTION

2.1   Deaberration

Adaptive imaging, or deaberration, is needed and used in many media, notably the atmosphere, ionosphere, solid earth, and oceans. In each case the methods used depend essentially on the nature of the aberrating medium: its spatial/temporal scales, nature of scatterers, access to the medium or surrounding volume, possible point targets in the medium, dispersive, refractive, and reflective properties of the medium and its interfaces, and attenuation. In these respects ultrasound is like no other medium, but exactly what it is is hard to pin down, in spite of much intensive work by good people.

We begin our remarks on deaberration (Section 3) by reviewing what is known to us about these physical characteristics of the tissue medium, following on some introductory remarks in this direction made in our last year's report (JASON report JSR 94-120). Some puzzling questions arise. For example, it is stated [1] that the total aberration phase shift across a typical linear array (128 elements) is less than one wavelength in certain tissue, yet similar tissue is reported to have Rayleigh-distributed amplitude fluctuations [2]. The former property is consistent with weak scattering, and the latter usually is not thought to be. However, amplitude fluctuations in a tissue medium can happen because of the strong intrinsic attenuation of tissue which comes about via mechanisms not related to elastic scattering,

including viscosity and coupling to transverse or surface modes. These attenuation mechanisms can vary strongly as a function of position in the tissue and of frequency. More attention needs to be paid to this physical (as opposed to diagnostic) characterization of tissue; a good example of what can be done is the work of Rose et al. [3]

Section 4 contains some remarks on deaberration in a hypothetical tissue medium which is consistent with, but not demanded by, the characteristics reviewed in Section 2.

One of the interesting developments of the last few years in ultrasound is the idea of time reversal [4], in which a point target in the tissue (for example, a kidney stone) is insonofied. The aberrated return is sensed and then time reversed, yielding in practice a good focus on the target. (Attenuation effects, which interfere with time reversal invariance, can usually be compensated for.) In the presence of point targets of varying brightness, it is possible to iterate the basic process and find good focusses on each target as well as on the neighborhood of the target. Clearly there is potential use for time reversal in deaberration if suitable point targets can either be found or made (with contrast agents or by sharp focusing of a transmitter beam on a good reflector). This subject is discussed in Section 5.

2.2   2D Transducers

The problems of making a large (say, greater than 100×100) 2D ar-

ray are well-recognized in the ultrasound world: connecting the channels to equipment outside the transducer module, processing the data at high rates if video-rate images are to be made, and dissipation of power from electronics in the transducer module. If the transmitter and receiver are physically identical piezoelectrics there are power problems not only in transmission but in the receive electronics.

In Section 6, we cover some ways of getting around these problems and of extending the use of large 2D arrays. Our notional system has a basic configuration modeled on an infrared bolometer array (we discussed the use of infrared array technology for ultrasound briefly in last year's report). The receiver and transmitter may or may not be physically separate; if disjoint, the combined arrays can be used in multistatic arrangements for deaberration purposes and one is freed from the necessity of using piezoelectric material in the receive array. We discuss some alternative receiver concepts, including capacitive microphone arrays. We size the data rates and receiver electronics power requirements for two systems at opposite ends of the data-rate spectrum: one capable of capturing the complete time-dependent RF signal from every one of the ten thousand or more pixels in each ultrasound pulse, and one operating confocally and picturing one voxel per ultrasound pulse. In the first case the data rates and receive electronics power are daunting, but a worthwhile goal for the ARPA program; in the second case the data rates are essentially trivial by today's standards, but it takes 2.5 seconds to make an image on a 100×100 array. The second system makes use of track-and-hold circuits and multiplexers to time-divide the output data to fit the round-trip pulse travel time, and uses only 100 A/D converters. (This sort of technology

19

is already in place in a JPL project to develop a small cheap TV camera, discussed in another JASON report). One can envision many systems lying between these two extremes.

One important consumer of power in such large arrays are the A/D converters. Some A/D converters otherwise usable for ultrasound receivers dissipate power at the level of watts, which would make them unacceptable in large arrays using one A/D converter per pixel. But much lower-power A/D converters can be built and are in use; the JPL TV camera cited above uses a total power of only 35 mw and has 176 A/D converters. Section 7 discusses some of the ways in which low-power A/D converters can be designed and built.

2.3 What This Study Does Not Cover

Given our limitations of time and knowledge, it is impossible for us to cover all of the interesting developments and prospects for ultrasound deaberration and large 2D arrays. This by no means implies that we find these subjects less interesting, or of lower priority in the ARPA program. We give explicit mention to some of these concepts here, which are otherwise not discussed in detail.

It will be important to develop image understanding and knowledge-based systems for ultrasound, both to assist in the technical process of de-aberration and to make ultrasound tissue images more accessible to non-

radiologist medical personnel. Equally important will be the development of telemetry so that images produced by a non-radiologist can be immediately transmitted to an radiologist expert for interpretation. These issues will be of particular concern for battlefield front-line care, and have been supported by ARPA in the past; continuing attention to them is necessary.

In 2D transducers we have paid little explicit attention to transmitter technology, but this is a subject of concern just as much as for receivers. One particular issue is the efficiency of piezoelectrics, which becomes more important as arrays get larger and need more power. There are many ways to split up the burden of providing adequate sidelobe rejection between the transmitter and receiver if these are not the same apparatus; these might involve different levels of sparseness or apodization. Sparse arrays, considered in themselves, are deservedly of much interest in the ultrasound community now and need further research.

Finally, there are a number of research areas, long pursued in ultrasound, which could support deaberration and/or diagnosis in various ways. These include sonoelasticity [5] and other elastic-mode studies; frequency-domain effects; and non-linear effects such as harmonic generation and coupling to transverse or surface modes.

3 OBSERVABLES IN ULTRASOUND IMAGING

3.1 Ultrasound Propagation In Tissue

3.1.1 Introduction

An acoustic wave impinging on a complex medium such as the human body from a specific direction undergoes refraction, diffraction, and scattering on its way through tissue. To first order, refraction is caused by sound-speed variability with scale sizes much larger than the Fresnel length, scattering is caused by objects much smaller than the acoustic wavelength, and diffraction enters in the intermediate regime. Human body tissue at ultrasound frequencies has another important property that complicates the analysis: intrinsic attenuation that may vary strongly with position.

Ultrasound may be compared with other applications in which waves traverse complex media. In particular, adaptive optics for ground-based telescopes has much in common. However, there are major differences in the two media that make transfer of adaptive techniques very questionable and require substantial research at this point. The differences are:

- The intrinsic attenuation in the atmosphere is negligible, whereas in human-tissue ultrasound it is very high.

- The fractional variation in index of refraction in the atmosphere with

scale sizes near the optical wavelength is less than a percent, whereas in ultrasound it is measured in the tens of percent.

- In the atmosphere the regions of differing levels of turbulence are not separated by sharp interfaces, whereas the human body is separated into regions (bone, organs, muscle...) by sharp interfaces.

In traditional ultrasonic imaging we are observing the backscatter cross-section from each "voxel" (volume element). Our image consists of a display of the estimated backscatter cross-section on some surface through the anatomical part being observed. The image depends on the coherent addition of all the array elements, range gated to account for different travel times from the voxel.

It is important to realize that a traditional ultrasound image is **not** really like a radar image. A radar is emitting into what is mostly empty space, and only a few objects (aircraft) return any energy whatsoever. On the contrary, ultrasound is emitted into a space filled everywhere with backscattering tissue of one kind of another, and with larger or smaller cross section. Therefore, the energy associated with a voxel has some contribution from many other voxels: so many others that even though each "wrong" voxel contribution is small, their sum is comparable to the total contribution of the "right" voxel. As a result, contrast ratio in ultrasound is **intrinsically low**.

In order to deal with this low contrast, ultrasound depends on the use of the "confocal" technique. Each voxel is illuminated by the transmitter

focussing as best it can on that voxel. Then the return is observed in the receiver array. If this confocal method were not used, ultrasound images would be useless.

It is also important to note that often the strong returns in an ultrasound image are often unimportant; the weak returns carry the needed information. (For example, the blood flow rate in the heart is not as important as the changes in heart-wall thickness during a heartbeat.)

A number of the points made in this section were also made in our report of last year [6]; this year we have more confidence in a number of statements because of discussions with more of the researchers in the field, and because of attendance at conferences on the use of ultrasound in medicine. We now discuss the overall phenomenology of effects on ultrasound propagation and scattering in human tissue.

3.2 Large-Scale Variability

Let us start with information about the large-scale features of tissue that are traversed with an ultrasound beam. This is a problem in tomography. Tomography has two aspects; these aspects are illustrated by applications in X-ray tomography (CAT scans) and ocean-acoustic tomography. In a CAT scan, the X-ray beam is known to follow a straight line through the medium, and the property of the medium being imaged is the absorption coefficient along that straight line. In ocean acoustic tomography, the medium does

not absorb significantly, but the changes in the sound-speed field cause the beams of sound (geometrical-acoustics rays) to move in space depending on the field of sound speed being hypothesized in the tomography algorithm. Those fields of sound speed are smoothly varying in space. In ultrasound, both effects are present, and in addition, the fields of sound speed are made up of large scale features separated by sharp interfaces.

The large-scale features represent the boundaries between organs, muscle, collagen, and bone. Present ultrasound systems assume that features of this sort don't exist; there is only a uniform sound speed with small-scale variability superposed. We consider it likely that a research program aimed at measuring the large-scale variability with tomographic techniques will allow the removal of significant aberration before moving down in scale size to remove the effects of diffraction. The major hurdles to overcome in applying tomography to the ultrasound situation are two of the above-mentioned effects: large attenuation and sharp interfaces between large-scale features.

We also want to emphasize that if these large-scale features are treated correctly, then the algorithms that come later and which are expected to remove aberration due to small-scale variability may work substantially better. This is an important direction for research, and it is one that could be investigated in the beginning by the use of numerical simulations.

We note some research done in the area that correctly associates what are labelled "artifacts" as coming about because of refraction at sharp boundaries [2]. These studies comprise what would be called "the forward problem", and are anticipatory of tomography efforts to invert such measurements

for the actual interior structures.

Because of the differences cited above, tomography will not simply be a translation of already-known techniques to the ultrasound application. Other media that use tomography have the characteristic that the large-scale variability is smoothly varying across the volume of interest, and a relatively small number of sources and receivers can be used to extract that variability. In the ultrasound situation the boundaries between organs and between organs and bone are sites of substantial change in sound speed (tens of percent) over a very small distance. Such boundaries not only prevent the use of smoothly turning geometric-optics rays, but they also introduce reflection, which is not in evidence at all in other fields. Therefore this is an area in which significant new research needs to be done. The only area that has many of the same characteristics is seismic exploration. It is possibly of interest that the seismic-exploration field chooses to put its sources and receivers in a long line, so that each scattering point is viewed from a number of bistatic angles, not just backscatter.

Another important research effort is combining CT scanning of the skull with ultasound imaging of the head. The top of the head is a good place to start because the skull is particularly simple, so the removal of its large-scale effects seems promising.

3.3 Intermediate-Scale Variability

A number of measurements have been made of the arrival-time variations over short length scales that are incurred in traversing tissue.

- The variation in travel time through a 1.5-cm section of abdominal wall has been measured to be of order 50-100 ns by one group [7], and up to 1 μs by another [8]. Measurements across the female breast yielded similar results: $\approx$50 ns by one group [1], but also some results with much larger variations of 1-2 μs [9]. Measurements in liver tissue yielded small variations in travel time [8]. The wave period of 5-MHz sound is 200 ns, so that in the typical ultrasound application at 3-5 MHz these variations can vary from much less than to much greater than one cycle.

- The transverse coherence length of this travel-time fluctuation was measured as somewhere between 2 mm [10, 1] to 5-10 mm [7].

- The amplitude, or intensity, of the waves has been measured to vary much more than expected from a weak-fluctuation perspective. In very strong fluctuations the intensity of a wave that has traversed a random medium takes on a Rayleigh distribution [11], whose rms value is 5.7 dB. Amplitude variations that have the Rayleigh character have been observed in at least two cases: one observed a Rayleigh distribution in the presence of large arrival-time fluctuations (1-2 μs) [9], whereas the other observed large intensity fluctuations (5 dB rms) in the presence

of small arrival-time fluctuations (70 ns) [7].

- We remark here that the measurements cited above are mainly made with one-dimensional transducer arrays that average over one of the transverse dimensions. This average is taken over a length that is typically 10 mm. As a result much of the information provided may be misleading. One of our main recommendations is that two-dimensional arrays be built so that a true three-dimensional analysis may be made.

We can now ask ourselves whether we can develop a picture of the tissue inhomogeneities in the human body that can be consistent with these measurements. This was begun in last year's report [6], some parts of which we incorporate into this section for convenience. We can remark first that the observations showing a Rayleigh distribution of amplitude while simultaneously having much less than a cycle of travel-time fluctuation cannot be understood in the context of a medium without intrinsic attenuation variations. Thus analogies with atmospheric adaptive optics must fail if those experiments are verified.

However, it should be possible to develop a theory with intrinsic attenuation variability using the same mathematical and numerical techniques that have been used in adaptive optics; the support of the development of such a theory is one of our recommendations.

Suppose we reject those observations and assume that the observations of arrival-time fluctuation rms values of about 50 ns are reasonable. Then we can use some simple models to determine certain aspects of human tissue.

Let us define:

C_o = average wavespeed ≈ 1500 m s^{-1}

μ_{rms} = root mean square of $\frac{C - C_o}{C_o}$

$(\Delta t)_{rms}$ = root mean square of travel time through tissue

D = thickness of tissue

L = correlation length of sound-speed in tissue

λ = ultrasound wavelength

f = ultrasound frequency

q = ultrasound wavenumber = $2\pi/\lambda$

R_f = Fresnel length = $\sqrt{\lambda D}$

r_o = acoustic coherence length

Using a single-scale, isotropic model of sound-speed fluctuations, we find an rms fractional soundspeed fluctuation to be [11]

$$\mu_{rms} \approx \frac{C_o(\Delta t)_{rms}}{\sqrt{LD}} \qquad (3\text{-}1)$$

As a result we find for abdominal wall [7]

$$\mu_{rms} \approx 1.0 \times 10^{-2}. \qquad (3\text{-}2)$$

whereas breast tissue measurements give results that vary from being similar to being larger by up to an order of magnitude [2].

The correlation length L of sound-speed variations in human tissue is related to observations of acoustic-field coherence length by the following equation that again depends on a single-scale isotropic model:

$$L = q^2(\mu_{rms}^2)Dr_o^2 \qquad (3\text{-}3)$$

Take the following numbers: 5 Mz, 50-mm range, and 5-mm coherence length for an observed field. These numbers yield a correlation length of 50 mm, or ten times the observed coherence length of the field. This is because the focussing and defocussing properties of the tissue make the acoustic field more and more fine-grained as the field pushes further into the medium.

Finally, considering frequencies in the range of 3-10 MHz we find an rms phase fluctuation of 0.2-0.5 cycles. These values imply that using weak fluctuation theory will often not be adequate, and that strong-fluctuation theory is not valid either [12]. This regime provides the perfect application of numerical simulation on present-day accessible computers. Needed research in the area of intermediate-scale tissue variability could concentrate on the measurement of a wide variety of tissue samples from a variety of organs; these measurements should allow for anisotropy of the variability in three dimensions, and include scales sizes from the wavelength of ultrasound (down to 0.1 mm) up to larger than the Fresnel length (3-5 mm).

These sound-speed fluctuations limit the resolution capability of ultrasound equipment. The effective resolution limit can be understood by asking for the rms tilt of a wavefront passing through tissue. Let Θ_{rms} be the rms tilt in one coordinate. Then

$$\Theta_{\mathrm{rms}} \approx \frac{C_o(\Delta t)_{\mathrm{rms}}}{L} \approx \mu_{\mathrm{rms}} \sqrt{\frac{D}{L}} \approx 10^{-2} \sqrt{\frac{D}{L}}. \qquad (3\text{-}4)$$

It is difficult to pick values for D and L because there is so much variability. However, we can estimate that values for Θ_{rms} can vary from a fraction of a degree to several degrees. Since the resolution of an array is $\Theta_{\mathrm{rms}} = \frac{\lambda}{l}$ where λ is the wavelength and l is the length of the array, our Θ_{rms} limits

the coherent array lengths in ultrasound to:

$$l_{\max} \approx \frac{\lambda}{\Theta_{\mathrm{rms}}} \approx 10 - 100\lambda. \qquad (3\text{-}5)$$

Since arrays are typically made with $\frac{\lambda}{2}$ spacings, to obtain optimal sidelobe suppression, we have determined that an estimate of the maximum useful number of elements in an ultrasound detector array is ≈ 100 per transverse coordinate.

The fact that ultrasound systems use broadband transmissions does not change this fundamental calculation; one simply uses the center frequency of the transmissions.

It is of interest to note that modern ultrasound receivers are already limited in resolution by sound-speed variations, since some of these receivers have ~ 100 elements in one dimension.

3.3.1   Amplitude Fluctuations

We note here that if amplitude fluctuations from focussing and defocusing were present, they would have a transverse coherence length smaller than that of travel-time fluctuations. Their typical scale would be a Fresnel length ($\sqrt{\lambda D} \approx 3$ to 4 mm) or smaller. The measurements of amplitude fluctuations have indicated very large values compared with expectations from wave propagation theory and a medium without intrinsic attenuation [7, 9].

If we take those measurements seriously, we must consider it a first-order

problem to clear up the question of their origin. Are they from intrinsic attenuation, and what spatial scales are involved in intrinsic attenuation in various tissues? Is it reasonable to see a "Rayleigh"-like distribution for acoustic amplitude when the usual reason for such a distribution (no intrinsic attenuation and strong phase fluctuations) is absent?

3.4 Small-Scale Variability

Variability on scales that are smaller than a wavelength generates a scattered wave field that emanates in all directions from the region of variability. One can usefully think of this situation as made up of discrete scatterers, and of the scattered wave as being distinct from the forward-propagating relatively unperturbed wave. Such variability does not affect the observations made in the very forward direction, and for the backscatter application one can separate the effects of the "scatterers" and the effect of refraction and diffraction that affect the propagation from the source to the scatterer and then again from the scatterer to the receiver.

The quantity of interest to the backscatter observations is the cross section for scattering per unit volume. One can break the scattering cross section into a number of separate contributions: scattering from very small point scatterers (like aerosols in the atmosphere), scattering from structures whose scale size is comparable with a wavelength, and scattering from smooth variations in sound speed on the scale of an acoustic wavelength. This latter contribution is equal to a simple constant of proportionality times the

spectrum of sound-speed variability at twice the acoustic wavelength. If one were looking at a region of relatively homogeneous tissue, then this cross section would have a certain value, whereas a region of pathological tissue might have a different cross section. In the past, tantalizing observations that seemed to indicate a difference between the cross sections of normal and pathological tissue have proven unreliable. Therefore our point of view here is that the cross section in backscatter provides the fundamental signal of an ultrasound observation, but we are looking only for spatial differences in that cross section within one patient, and not variations from some mean value over all patients or tissue samples.

If one has a specific model of microscopic structure in the tissue being ensonified, then one can calculate the backscatter cross section from first principles. An example of this type of calculation is contained in a recent paper about backscatter from myocardial tissue [3]. Those authors took as their model of each myocyte an ellipsoidal shell, and then took as their distribution of myocytes a random distribution leading to an incoherent sum. A further parameter of their model is the distribution of sizes of the myocytes. We shall see in the next section how that parameter can be used to fit the frequency dependence of scattering data. They concluded that their model is consistent with the observations of frequency dependence and anisotropy of the cross section.

3.4.1 Backscatter Phenomenology

The measurements of backscatter cross section from tissue in the 1-10 MHz range of frequencies can be described by a power law:

$$\frac{d\sigma}{d\Omega} = A \left(\frac{f}{1\,\mathrm{MHz}} \right)^n \qquad (3\text{-}6)$$

in which the units of A are $\mathrm{m}^2\ \mathrm{sr}^{-1}\ \mathrm{m}^{-3}$.

Last year we referred to a typical backscatter cross-section from homogeneous calf's liver as having a power-law index $n = 1.4$ for f between 3 and 10 MHz [13].

This year we can add new sets of data for myocardial tissue that have quite a different frequency dependence [3]: namely, n between 3 and 4. Therefore it becomes important to know which tissue one is encountering in predicting the expected behavior with respect to frequency.

In last year's report the experimental power-law index was interpreted as a measure of the slope of the spectrum of inhomogeneities in sound speed at the appropriate wavelength.

An alternate and equally useful interpretation is taken by Rose et. al. [3]. They use a parametrized distribution of myocyte sizes to obtain the power-law index in the backscatter cross section. In either case the phenomenology can be used with the proper number of parameters to represent the cross section. Finally, ultrasound image contrast is created by the difference between this homogeneous signal, and the larger or smaller signals

resulting from interfaces or voids, etc.

In last year's report we gave elementary discussions of the attenuation and the smoothly varying sound-speed model that could be used in parametrizing the data. Here we just note again that the intrinsic attenuation is very strong (6 dB/cm at 3 MHz, proportional to frequency) and that the use of the observed backscatter cross section to set the variance of the sound speed fluctuations results in sound-speed variances consistent with the direct measurements.

3.5 Summary and List of Promising Research Directions

The above analysis illustrates the tight relationships implied by variable soundspeed as a model for the source of ultrasound scattering and attenuation. We see that there is an obvious lack of sufficient data to formulate a realistic model of the medium at this time. One obvious point is the lack of understanding of the origin of the large observed amplitude fluctuations. There is also no systematic data base on the properties of different types of tissue. Only a few measurements at a few frequencies for a few tissue types (abdominal wall, breast, liver) have been carried out. Only backscatter has been considered seriously rather than bistatic geometries. All of this information would allow more precise system design. Finally, a model for interfaces between tissue types is needed to predict contrast ratio in real ultrasound images.

We suggest that attempts to improve ultrasound images should start from the fundamental physics described here and first do a reasonably complete set of fundamental measurements of tissue properties. At the same time studies may go ahead in numerical simulation using possible tissue characteristics in order to provide quantitative predictions for the performance of possible systems.

The following list of promising research directions comes directly out of the discussions in this section:

- Determine the spectrum of inhomogeneities of various types of tissues, including variability between organs and between patients in the same organ. This is a three-dimensional effort involving looking for anisotropy.

- Develop a research program aimed at measuring the large-scale structure of a patient's sound-speed structure (tomography). This large-scale structure must be allowed to have very sharp interfaces between sections. Overcome the difficulty of not having tomographic straight-through propagation in most of the available acoustic paths.

- Determine the source of the large variations in acoustic intensity observed in ultrasound experiments. Some of those same experiments indicated small variations in acoustic arrival time; the combination implies that there are strong variations in intrinsic attenuation in human tissue. Other experiments had large arrival-time variations. Can they both be correct?

- Support numerical simulations of wavefront and/or phase distortion from various models of inhomogeneities that are consistent with the experimental results (including *both large and small scale variability* that have been determined so far. (Neither weak nor strong fluctuation theory are appropriate.)

- Develop two-dimensional transducer arrays with at least 100×100 elements for both transmit and receive so that the ultrasound information can be analysed in terms of three-dimensional inhomogeneities.

4 ON DEABERRATION

We have covered in the last section some of the physical manifestations
of aberration in both one and two dimensions. Here we will discuss how
these are or are not corrected in certain deaberration schemes (e.g., time-
delay compensation [14] and the closely-related principle of phase aberration
correction [15]); how these schemes are related to ad hoc tissue models; and
the general question of whether deaberration should be done with model-
based schemes or figure-of-merit schemes which try to improve some sort
of global sharpening factor, as is common in astronomical adaptive optics.
We will not discuss image improvement by speckle averaging or the use of
beacons (Section 5 discusses time reversal, which uses in-tissue targets). The
tissue model implicit in time-delay or phase-correction schemes is that of a
single phase screen; if backpropagation corrections are used, the phase screen
can be deep in the medium. The trouble is that this is not a very realistic
model of most tissues, and really does not do well in correcting for large-scale
refractive effects. A figure-of-merit scheme is less commonly considered since
many of these require in-tissue beacons. The result is that deaberration as
practiced today is largely unsystematic and empirical. Perhaps this is all it
ever will be, in view of the intransigence of the tissue medium, but one ought
to try a little harder.

4.1 Time-Delay Compensation and Backpropagation

In time-delay compensation (or phase aberration correction) one cross-correlates the pulse returns on neighboring elements (or maximizes speckle brightness) to find time shifts which are applied to the return pulses to compensate for medium-induced distortions. Clearly this will work perfectly if the imaged medium is homogeneous with uniform sound velocity except for a phase-aberrating screen placed next to the receive array.

In fact, phase compensation does not work perfectly because the tissue medium is not a phase screen on the transducer. Another model [16] allows for a single phase screen (aligned with the transducer) at any distance from the receiver in a homogeneous medium, and then computes propagation corrections to phases and amplitudes after locating the phase screen (see Figure 4-1 for the general idea). But the medium is not a single phase screen wherever located. Nevertheless, Liu and Waag [16] claim improvement over pure time-delay compensation in human abdominal wall tissue, which might arguably be represented as a phase screen represented by the fascial and muscle layers near the surface.

Let us continue for the moment to make the phase-screen-at-a-distance hypothesis, and ask, as Krishnan et. al. [17] do, what is the effect of simple time-delay correction for a remote phase screen. (These authors then go on to a method called the parallel adaptive receive compensation algorithm, or PARCA, which attempts to do some amplitude deaberration based on a
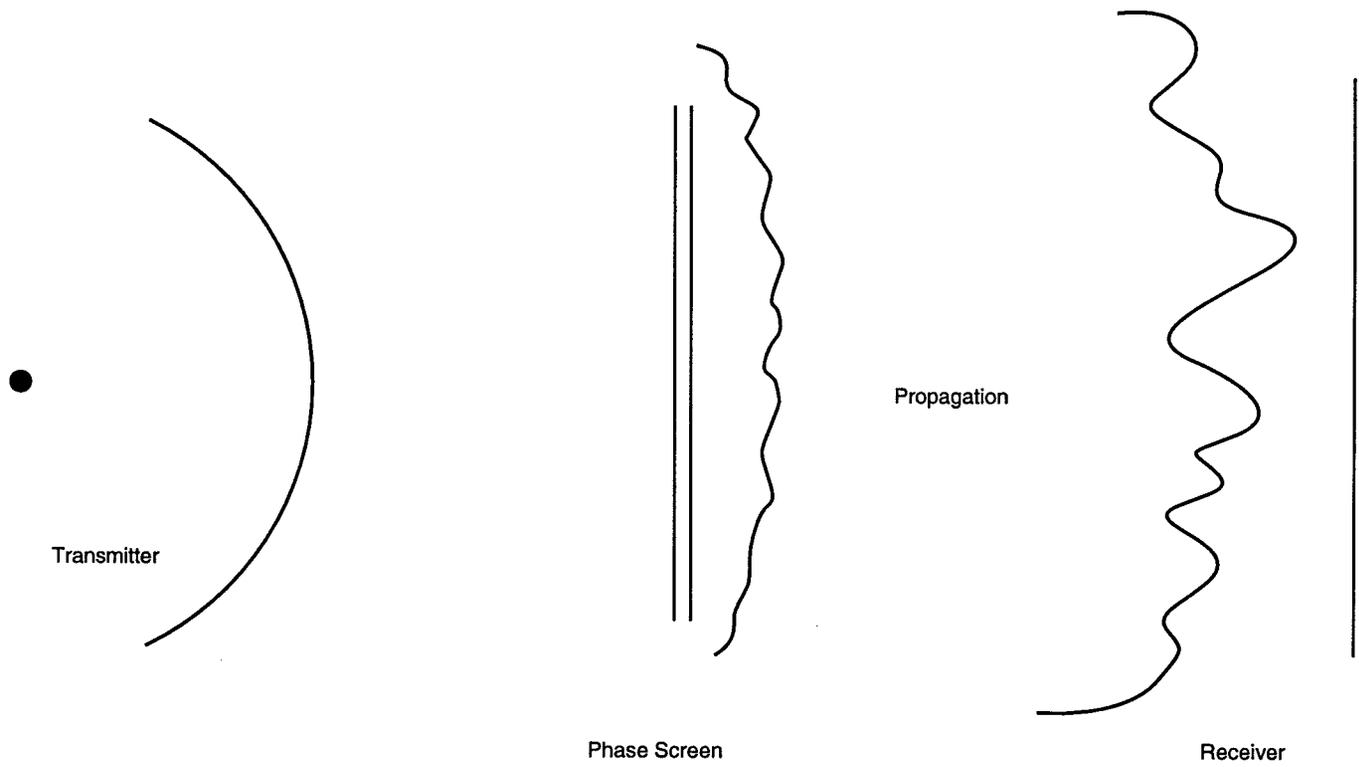
Figure 4-1. Effects of a distant phase screen and propagation in aberration.

least-squares criterion; for the moment, that is not the issue here.) Krishnan et. al. have made a computer simulation of such a screen. The parameters for the simulation specified a 128-element linear array with a center frequency of 3.75MHz and bandwidth of 40%. A point source was introduced 10cm away, and the phases screen was 0.8cm in front of the transducer. Figure 4-2 shows several aspects of the simulation: Figure 4-2a shows the phase aberrations introduced by the phase screen (and thus what would be measured on the array if the two were spatially colocated). Figure 4-2b shows the actual phase aberrations measured; the discrepancy is due to propagation (Figure 4-1). Note that the phase shifts on the screen are large but not so large as to put one in the regime of strong scattering.

Figure 4-2c shows that propagation has introduced amplitude modulations as well, ranging up to a factor of 2. This figure is normalized to unit relative amplitude in the absence of the phase screen. These perturbations are on a scale of a few wavelengths (one element number corresponds to half a wavelength), and are sufficient to introduce large perturbations in the correlation of signals between the first and the Nth element (Figure 4-2d). One should note here that these decorrelations are large compared to the decorrelation which would be seen if speckle were the only source; the Van Cittern-Zernike theorem [18] essentially says for our conditions that the correlation length associated with speckle is determined by the array size. Amplitude perturbations on the scales shown in Figure 4-2c will degrade the resolution.
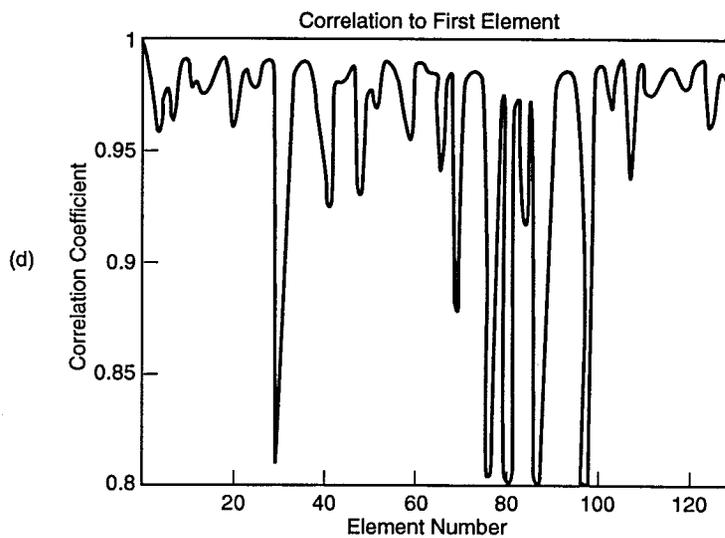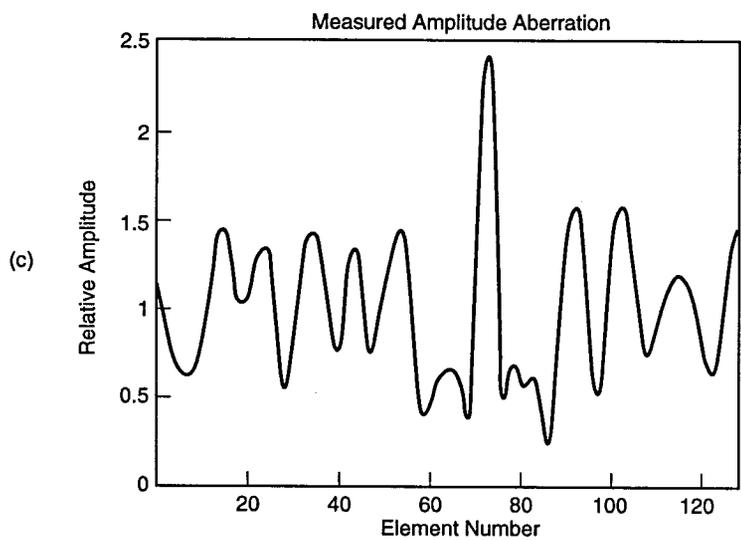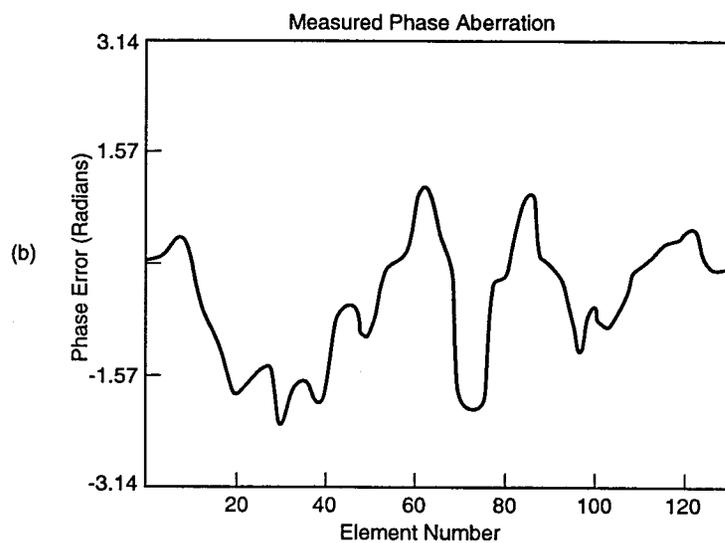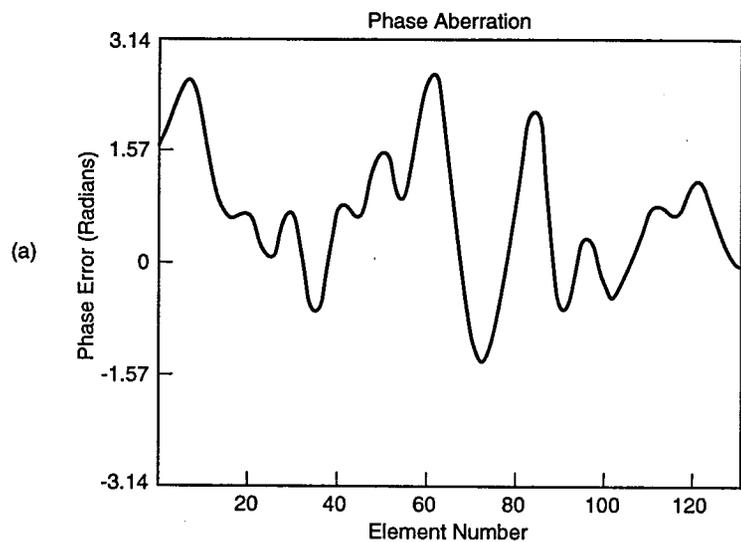
Figure 4-2. Phase-screen simulation (from Krishman et al. 1995).

4.2 Phase Screens and Phase Tomography

One can now imagine inventing more complicated and conceivably more realistic tissue models based on more and more phase screens, always assuming constant-speed straight-line propagation between screens. The more screens the more measurements needed to disentangle them. One way to try this is with a tomographic method based on limited angular diversity of measurements, as illustrated in Figure 4-3. The orientation of the transducer with respect to the tissue blob is given by the angle ϕ, and u is a distance along the transducer specifying a beam line. As u and ϕ are varied one measures, in the phase-screen approximation, the quantities

$$\int dx dy k n(x,y) \delta(x \cos(\phi) + y \sin(\phi) - u) \tag{4-1}$$

where the index of refraction n is a sum of delta functions specifying the location of the phase screens in the slice (x,y) plane times the random component of the index corresponding to each screen. Propagation (diffractive) effects are not included in Equation (4-1) Given complete coverage in u and ϕ, one could invert Equation (4-1) to find n by standard tomographic techniques [19, 20] but one does not need complete coverage given the model of n as a series of phase screens. We will not discuss here the precise requirements of coverage in u and ϕ for untangling the phase screens, but it should be clear that the more data the more complicated the tissue model can be. Of course, since no tissue is a series of phase screens, the image cannot be completely deaberrated this way, but it might happen that further application of a figure-of-merit-based technique or some other empirical approach

44
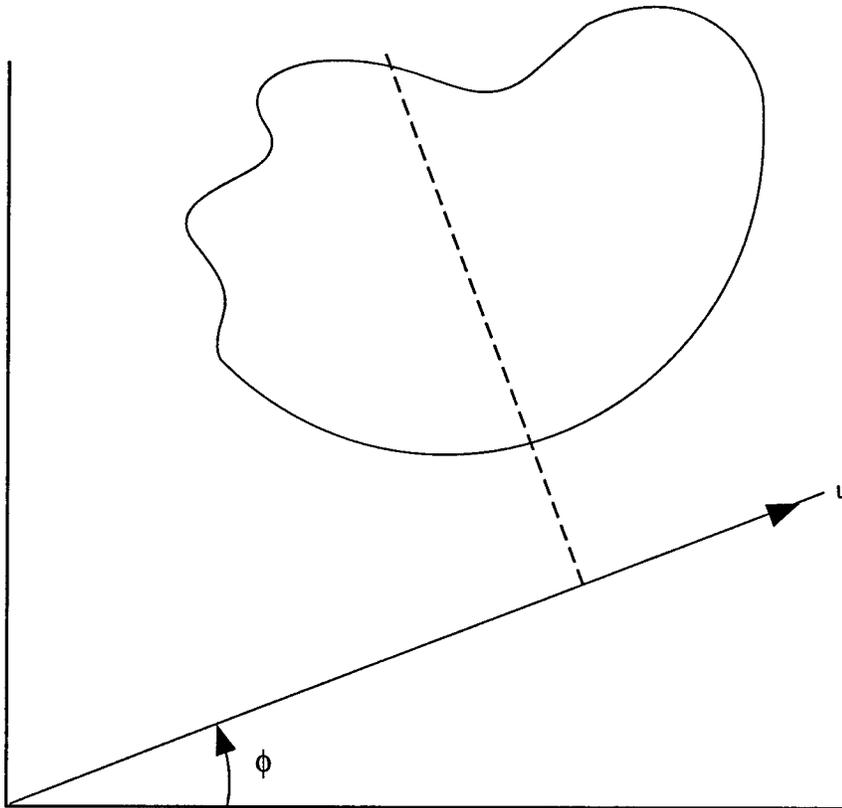
Figure 4-3. Setup for phase tomography.

help even more than it does for a single screen model. This is a more complicated version of the general idea behind time-delay and related compensation schemes:

- Invent a deaberration scheme which works perfectly on some idealized tissue model, which may not be very realistic;

- Try it on real-world tissue data to see how well it works;

- If it doesn't work all that well, improve it empirically based on some figure of merit.

4.3   Models or Figures of Merit?

A model approach assumes some parametrization of the imaged tissue, then attempts to find those parameters from the aberrated image. A figure-of-merit approach, at least for the present purposes, is one which attempts to deaberrate the image without ever calculating any of the parameters of the medium. The ultrasound deaberration problem is very difficult, so that realistic but tractable tissue models are hard to come by, and figure-of-merit approaches typically need point targets in the tissue, also hard to come by. The result has been that neither modeling nor figures of merit have helped very much in deaberration.

Given no *a priori* model of the medium, one must do inverse scattering [21], [22], [23]. But inverse scattering is always difficult, often ill-conditioned,

and in principle requires complete coverage in such variables as u and ϕ introduced above. An initial model of the tissue being imaged is very useful in overcoming all these limitations, but if the model is not realistic and faithful it will not be of much use. We have no reason to believe that a multiphase screen model is at all realistic, or even any better than the one-screen model implicit in time-delay compensation. Still it might be useful to construct some simulations using (diffractive) phase tomography to see how it performs on computer-generated tissue models which are not just phase screens, and to see how increasing the number of sight lines does or does not improve deaberration.

We note that tomography has been used in the past [25] to measure sound-speed variations in tissue for direct diagnostic purposes; our suggestion is that tomography can be used as the first step in deaberration.

There are, of course, many other possible ways of using image diversity, short of full-scale tomography, to improve images. One such method, due to Y. Li, was described to us by D. Robinson [JASON briefing, 1995].

The trouble is that phase screens do not begin to model such real-world features as attenuation, refraction and multipath, and reflectors (bone, air). One might then use a figure-of-merit approach, where some global parameter depending on the received data is optimized (e.g., the sharpness of focus on a beacon). The problem is to find image features which can be used in the figure of merit, since beacons are not usually found in tissue. However, this problem is not altogether hopeless. In the specific ARPA context of battlefield care (or more generally in emergency medicine) the patient who is to be imaged may

require immediate medication of some sort which is injected into the body; such medication can include contrast agents to be used as beacons. Or a focused transmit beam can be used to provide a strong pointlike reflection from bone or other surface of acoustic discontinuity in the tissue. This will require good resolution in three dimensions, i.e., a high-resolution 2D array of f number near unity. We will say no more on beacons here (but see Section 5 on time reversal) except that their use ought to be reconsidered in deaberration.

A figure-of-merit approach often is combined with time-delay compensation to make corrections for propagation, amplitude changes, and the like. This is an empirically sensible approach but it leaves one in doubt as to where to look for systematic improvements on time-delay compensation. We would now like to suggest at least one direction in which to look.

4.4 Low-Frequency Modeling of Large-Scale Refraction

Refraction is one of the major causes of deaberration; it leads to multipath effects as well as loss of both contrast and resolution. It cannot be addressed in any model which assumes homogeneous straight-line propagation.

In Figure 4-4 we show results [2] of a transmission experiment over a distance of some 4cm through a water sample (Figure 4-4a) and a human breast (b, c). The transmitter is a point source and the water image shows
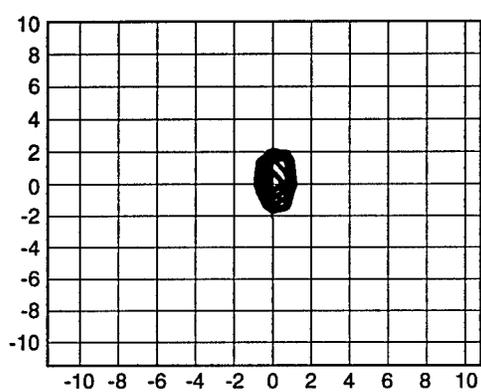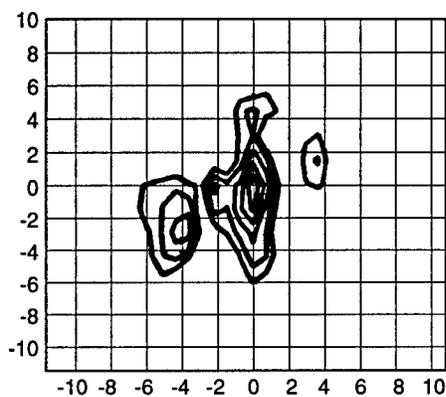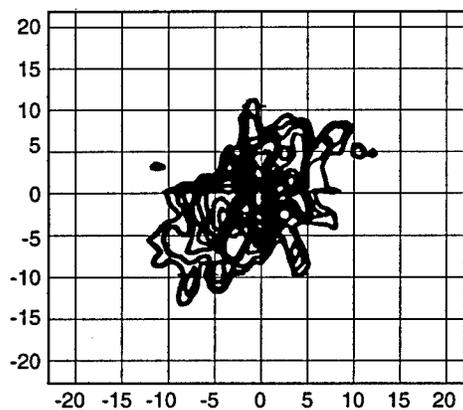
Figure 4-4. 2-D contour maps of point source images. (a) water data showing diffraction pattern of system. Outer contour is -10 dB level. (b) measured through the 4-cm tissue (brs006), showing highly asymmetric interference pattern. Outer contour is -10 dB level. (c) Image (brs006) at -16 dB contour level. The outer contour shows more symmetrical scattering pattern. Note the change of scale from (a) and (b). From Steinberg [briefing to JASON, 1995].

the diffraction-limited image of the source. At the -10dB level three distinct source images are seen (Figure 4-4b) and at -16dB the images smear into each other (Figure 4-4c). Zhu and Steinberg [24] applied both time-delay compensation and time reversal to these images, with some improvement (not shown here) in image quality but still with the multipath fictitious images present. These methods of deaberration are not correcting for refraction. Similar refractive effects are seen in images of other than breast tissue.

What can be done about refraction? To the extent that important effects come from objects of scale larger than a wavelength, perhaps quite a bit can be done. A multi-image technique using the Octoson eight-head scanner for deducing curved-interface refraction effects has been described [26]. Smith et. al. [27] tried modeling tissue as a series of tissue blocks each with a known homogeneous sound speed, separated by plane parallel interfaces; deaberration results were disappointing. A current program at CSIRO in Australia [D. Robinson, JASON briefing, 1995] with the acronym of STARS (subcutaneous tissue aberration removal scheme) uses an ordinary (4-6 MHz) ultrasound image to identify large-scale tissue volumes by type, assign them an *a priori* sound speed appropriate to the tissue type, and use straight-line (Snell's law) propagation to trace rays. This seems to be a worthwhile line of research to pursue, and we encourage it. If multipath effects can be tamed this way, perhaps time-delay compensation will work well to remove remaining image degradation.

If only large refractors are of concern, images made at low ($\leq$ 1MHz) might be even more useful than higher-frequency images [JASON report 94-

120, 1994]. There is much less attenuation (which is linear in frequency) and deeper penetration which would allow for partial tomography, if warranted. Furthermore, there is less data to process, which will always be a concern in deaberration going beyond time-delay compensation.

Clearly an important tool in any such program for dealing with refraction will be materially assisted by the image understanding tools ARPA has fostered in the past. These include assignment of tissue boundaries and types, displaying outlines and edges for assisting the viewer (especially the non-radiologist viewer) to understand the image, and providing other sorts of direct assistance to humans while at the same time serving as the input to deaberration software such as a ray-tracing program.

There are already applications of visualization techniques in ultrasound, especially for echocardiography and pre-natal obstetrics. J. Miller [JASON briefing, 1995] showed us his technique, now available commercially, for outlining the volume of the left ventricle as the heart beats, allowing for crucial quantification of blood-flow volume. Other applications of visualization in echocardiography are reviewed in Greenleaf et. al. [28]. Last year T. Nelson briefed us on three-dimensional surface-rendering techniques for fetal images [JASON report 94-120, 1994]. These are important, but at the moment we know of no image understanding techniques being used to remove refractive aberration.

4.5 Conclusions

Deaberration techniques currently lack *useful* realistic models of tissue, and so fall back on (if only implicitly) such props as phase-screen models. These are far from perfect, so that deaberration ends up being largely an empirical program. While it is unlikely that empiricism will ever be exorcised from this field, it seems to us that a better starting point which might conceivably reduce the empiricism is to make one or more (semi-tomographic) low-resolution images of the main tissue concentrations and their sound speeds, as interpreted with image-understanding tools and used as the input to other deaberration techniques. The deaberrated image, with image-understanding enhancements such as edge detection and tissue identification, will be useful not only to radiologists but (perhaps even more important for the ARPA battlefield care program) to non-radiologists.

5 TIME REVERSAL AND DISTORTION RE-MOVAL IN ACOUSTIC IMAGING

5.1 Introduction

The use of ultrasonic arrays for medical imaging would appear, on the face of it, to provide high resolution with little effort. With a nominal sound speed of 1550m/s an ultrasound imaging array operating at a center frequency of 2 MHz has a wavelength of 0.78 mm. For a beam emerging from an array of length D in some dimension focused at a distance Δ, two objects separated by order $\frac{\lambda \Delta}{D}$ should be resolvable. As $D \approx \Delta \approx$ a few tens of centimeters, the value of λ is quite relevant for the resolution available for clinical applications.

The images one achieves in practice have substantially lower resolution because the medium through which the sound propagates is inhomogeneous. There is significant distortion of both the amplitude and the phase of the acoustic signals making it difficult to interpret the images for medical or other identification purposes.

There has been no shortage of proposals for correcting this aberration [29]. Most have concerned themselves with readjusting the phase of the received acoustic wave to make it nearly planar, once known geometrical factors are accounted for, under the assumption that this will compensate for inhomogeneity in the medium if the distortion arises from weak scattering. This is equivalent to the assumption that directly in front of the receiver is a

"phase screen"—a fictitious medium which scrambles the phase of a wave by imposing random time delays to different spatial pieces of the wave but which leaves the amplitudes unaltered. These methods appear to concentrate on removing distortion in the phase of a sound wave presumed to originate from a point scattering source in the tissue. Assuming that the "correct" phase relationship would be that of a spherical wave emanating from this point source and then propagating through a homogeneous medium, the phases at the receive antenna are adjusted to meet this presumption. The adjustment is typically [30] a phase correction at neighboring receivers to make the phase on each pair of neighbors the same. The time delay Δt required to make this phase shift $\Delta \phi = \omega \Delta t$ is determined by the peak in the cross correlation function between the signal $s(i, t)$ received at the ith sensor and $s(i + 1, t)$

$$C_{i,i+1}(T) = \sum_t (s(i, t) - \bar{s}(i))(s(i + 1, t + T) - \bar{s}(i + 1)), \qquad (5\text{-}1)$$

where $\bar{s}(i)$ is the mean of the measurements of $s(i, t)$ over the integration time for receipt of the sound signal.

Other methods define quality factors such as the average speckle brightness and seek adjustments in the received signal to maximize this. The idea [31] is that speckle, the pattern of spots and dots appearing from a distributed set of scatterers in some medium, arises from coherent interference from the scattered amplitudes of many independent scatterers. When aberration is present, then the main lobe of the response of any given scatterer is diminished and the interference pattern shows decrease in its maxima. Compensation for the aberration or degrading in each scattered signal would be achieved by increasing the overall speckle brightness. Nock, Trahey, and Smith point out that aberration can actually increase the response from some

of the presumed many scatterers, so maximizing speckle brightness over the image may sometime lead one astray.

5.2 Time Reversal Acoustic Characterization of an Environment: TRACE

5.2.1 TRACE Elements

The work of Fink [32], Prada [33], and colleagues provides a refreshing and widely useful approach to the issues of removing aberration from acoustic images. They start with the observation that the acoustic wave equation for a medium without dissipation having density $\rho(\mathbf{x})$ and sound speed $c(\mathbf{x})$

$$\rho(\mathbf{x})\nabla \cdot \left(\frac{1}{\rho(\mathbf{x})}\nabla p(\mathbf{x},t)\right) = \frac{1}{c^2(\mathbf{x})}\frac{\partial^2 p(\mathbf{x},t)}{\partial t^2} \tag{5-2}$$

has both $p(\mathbf{x},t)$ and $p(\mathbf{x},-t)$ as solutions. Since the speed of sound is small compared to the speed of light, Fink, Prada and colleagues remarked that if one could measure the pressure wave $p(\mathbf{x},t)$ over some array resulting from a scattered wave from a set of objects, then by storing the pressure signals and rebroadcasting them after a time delay T but in reverse order to which they were received, namely $p(\mathbf{x},T-t)$, then the acoustic wave pattern would be refocused back to those scattering centers.

The manner in which this would work is shown in Figure 5-1. Here an array of N elements, possibly an area covered by M in one direction and M' in the other, $M\,M' = N$, first transmits a more or less arbitrary "probe" signal. The scattered version of this signal is recorded on the ar-

Transmit/Receive Array
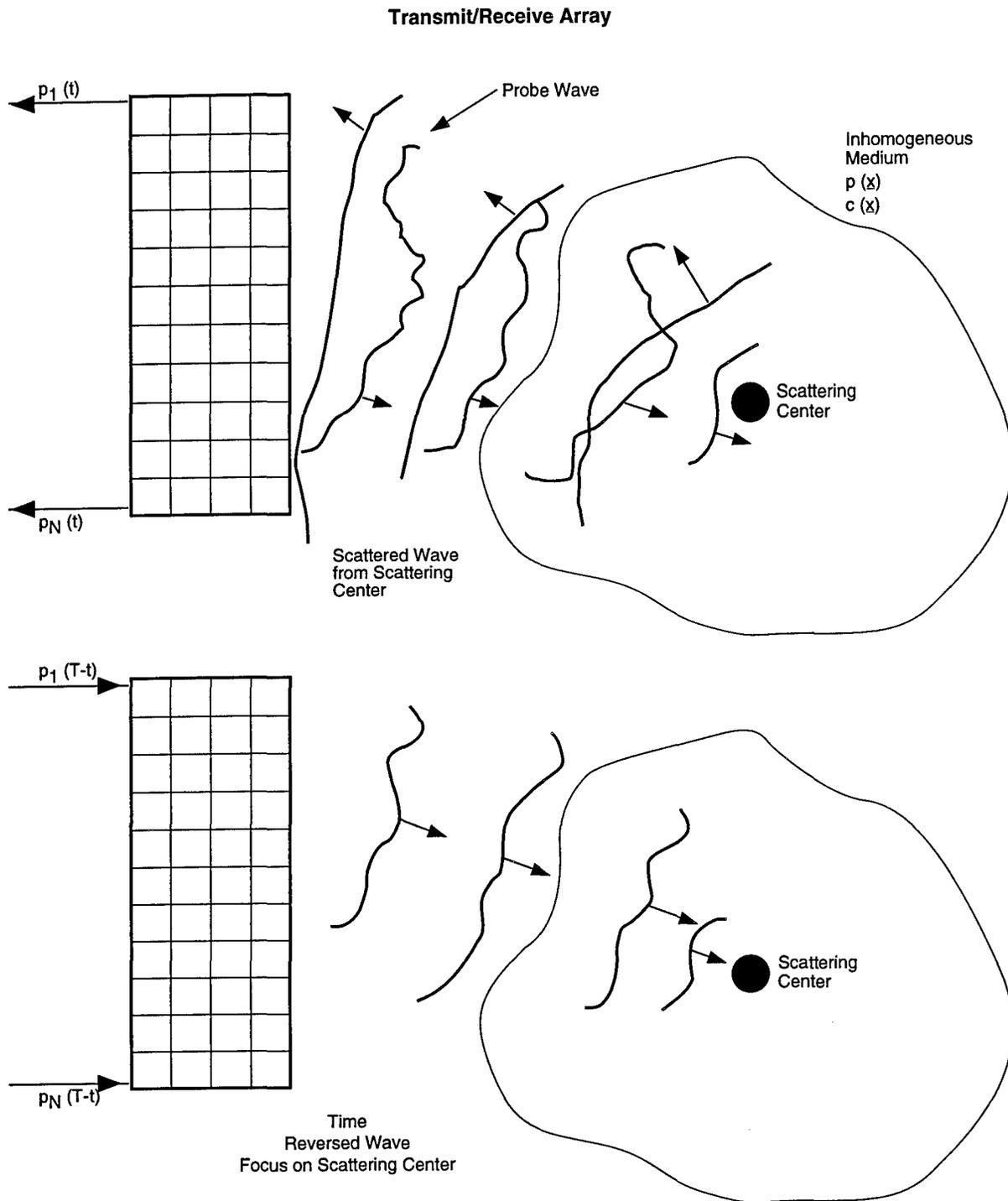
Figure 5-1.

ray as $p_1(t), p_2(t), \ldots, p_N(t)$, and stored over some integration time T. The signals are then rebroadcast from the same locations as $p_1(T - t), p_2(T - t), \ldots, p_N(T - t)$, and this series of signals sends the acoustic energy directly back to the scattering centers.

To rigorously and precisely refocus the signal back to its source, that is to turn outgoing waves $\frac{e^{ikr}}{r}$ from each center to $\frac{e^{-ikr}}{r}$ returning to that center, one requires a surface dense with transceivers, and that is not possible. In practice Fink's group has built several one dimensional arrays which accomplishes a very effective time reversed transmission of the received signals without trying to achieve the 'optimum'.

A practical mode in which one can use TRACE is to iterate the procedure just outlined. Suppose there are two scattering centers with cross sections σ_1 and σ_2 respectively. The returned pressure signal from the probe pulse will be proportional to

$$A\sigma_1 + B\sigma_2, \tag{5-3}$$

with A and B some constants. If the scattering centers do not insonify each other in a significant way, the return from transmitting a second time will be proportional to

$$A'(\sigma_1)^2 + B'(\sigma_2)^2, \tag{5-4}$$

and so forth for repeated time reversed retransmission of the received waves. If $\sigma_1 > \sigma_2$, the scattering from scatterer number one will soon dominate the return from the array, and that source of scattering will be imaged by the process.

Actually one can do more and focus sequentially on the strongest scatterer, the next strongest, etc. To achieve this consider the collection of signals coming from an impulse projected from each element of the array and then received by each other element of the array, at fixed frequency ω this collection of transmissions from element 1 and reception by element m is an N by N matrix $G_{lm}(\omega)$. The signal received at element m from any other emission $e_l(t)$ from element 1 would be

$$r_m(t) = \int_{t_0}^{t} d\tau \, G_{ml}(t - \tau) e_l(\tau), \tag{5-5}$$

back in time domain. In vector notation this can be written at frequency ω as

$$\mathbf{R}(\omega) = \mathbf{G}(\omega) \cdot \mathbf{E}(\omega). \tag{5-6}$$

Time reversal changes $t \to -t$ or $\mathbf{G}(\omega) \to \mathbf{G}^*(\omega)$—the complex conjugate. The matrix $\mathbf{G}(t)$ or $\mathbf{G}(\omega)$ is symmetric because of reciprocity [34]. On the first transmission of the signal $\mathbf{E}(\omega)$ the received signal is

$$\mathbf{R}_1(\omega) = \mathbf{G}(\omega) \cdot \mathbf{E}_1(\omega). \tag{5-7}$$

The time reversed version of this is

$$\mathbf{R}_1(\omega) \to \mathbf{R}_1^*(\omega) = \mathbf{G}(\omega)^* \cdot \mathbf{E}_1(\omega), \tag{5-8}$$

and is retransmitted into the target. On reception of this we have

$$\mathbf{R}_2(\omega) = \mathbf{G}(\omega) \cdot \mathbf{G}(\omega)^* \cdot \mathbf{E}_1(\omega). \tag{5-9}$$

After k iterations of this process, we receive the signal

$$[\mathbf{M}(\omega)]^k \mathbf{E}_1(\omega), \tag{5-10}$$

where the N by N Hermitean matrix $\mathbf{M}(\omega)$ is

$$\mathbf{M}(\omega) = \mathbf{G}(\omega) \cdot \mathbf{G}(\omega)^*. \tag{5-11}$$

The Hermitian matrix $\mathbf{M}(\omega)$ has real, positive eigenvalues $\lambda_a; a = 1, 2, N$ with associated eigenvectors V_a. In time domain these satisfy

$$\int_{t_0}^{t} d\tau \, \mathbf{M}(t - \tau) V_a(\tau) = \lambda_a V_a(t). \tag{5-12}$$

If there is a single strong scattering center in the target medium, then the return from that center is associated with the largest eigenvalue λ_1 of the matrix $\mathbf{M}(\omega)$ and the temporal pattern of pressure signals from this center is the eigenvector $V_1(t)$. The vector of pressure signals $\mathbf{E}(t)$ on the array can be decomposed as

$$\mathbf{E}_1(\omega) = \sum_{a=1}^{N} c_a \mathbf{V}_a(\omega). \tag{5-13}$$

If we iterate the time reversal process employing the matrix $\mathbf{M}(\omega)$, then after k iterations, the received signal is

$$\sum_{a=1}^{N} c_a (\lambda_a)^k \mathbf{V}_a(\omega), \tag{5-14}$$

and it is clear that the largest eigenvalue dominates after a few iterations.

What is equally interesting is that we can also focus on the next dominant scattering center by selecting the eigenfunction $\mathbf{V}_2(t)$ as the signal propagated from the array.

This effect is seen in Figures 5-2 to 5-4 where we see two wires with $\sigma_2 = 2\sigma_1$ ensonified by a line array, and in Figure 5-3, we have the returns as
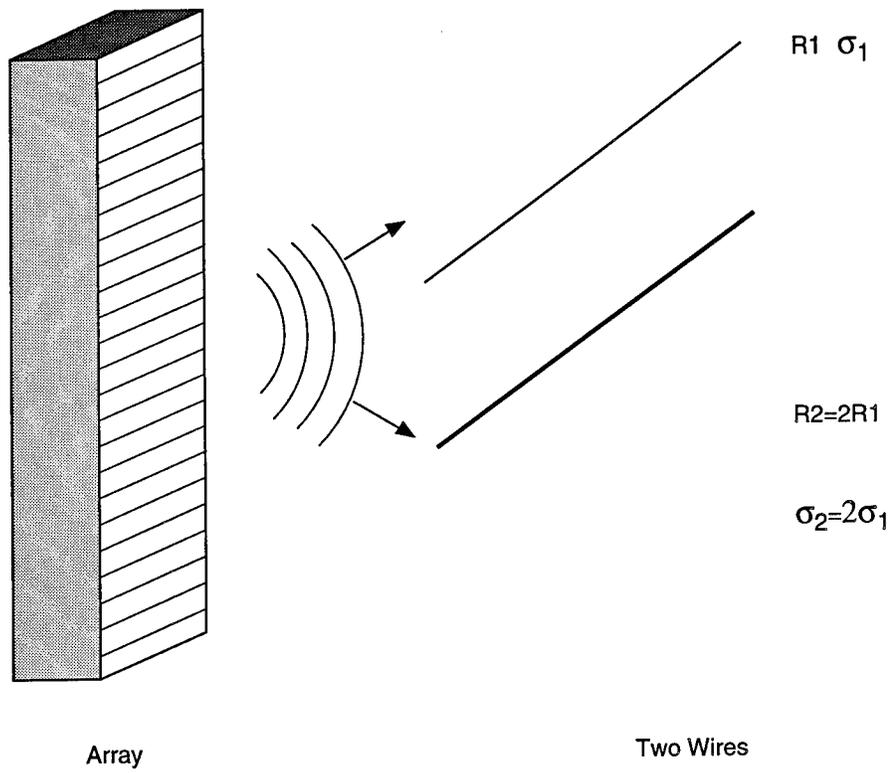
**Figure 5-2.** Time reversal experiment on two reflectors.
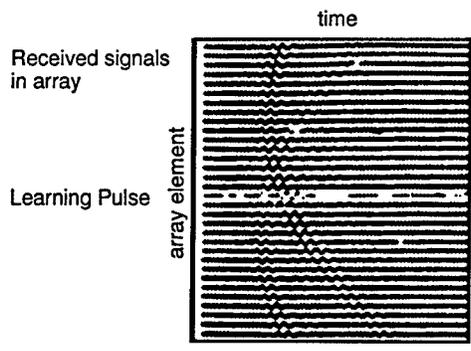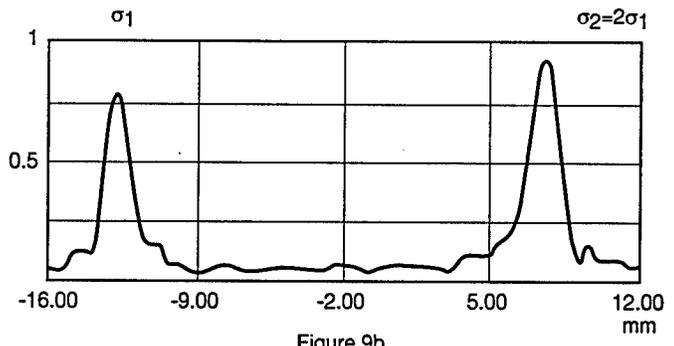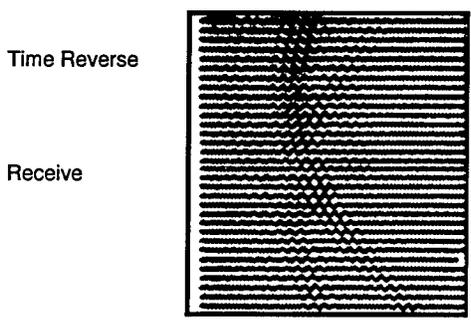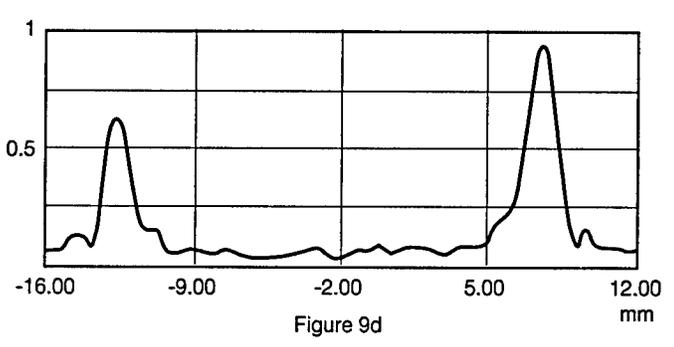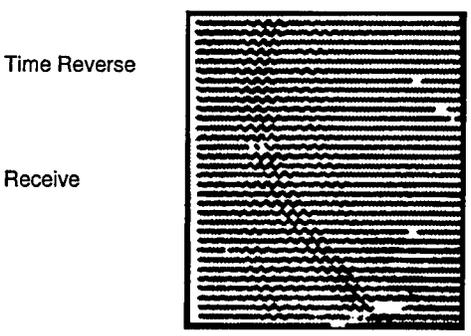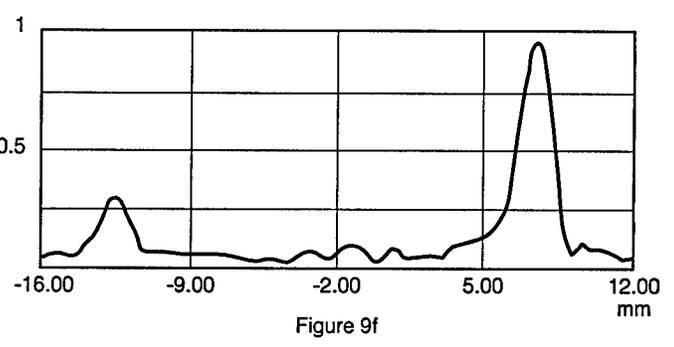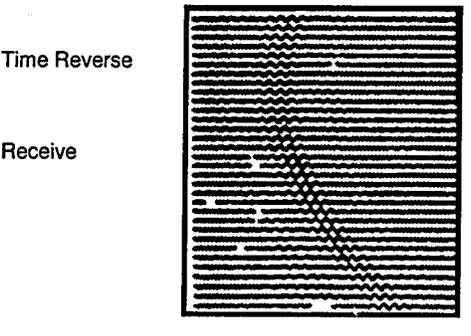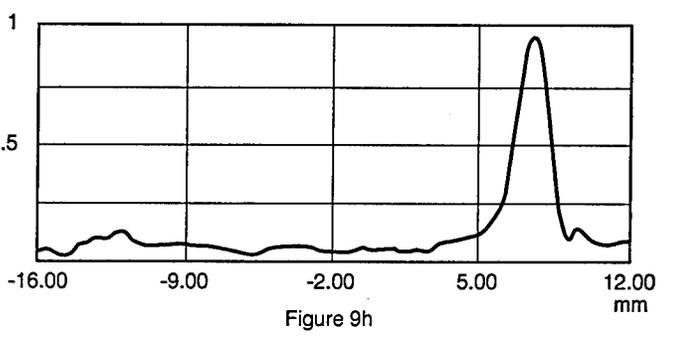
Figure 5-3. Linear array.
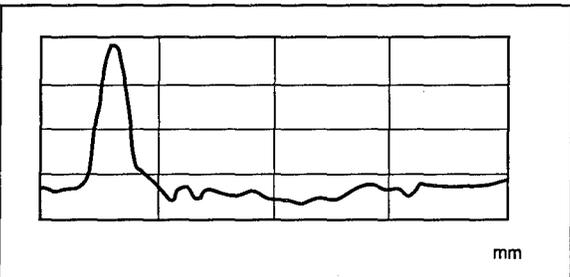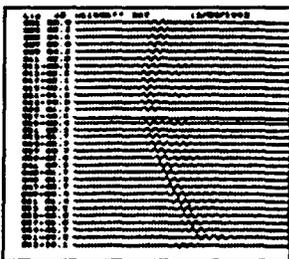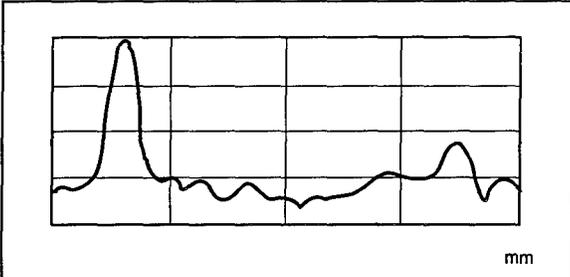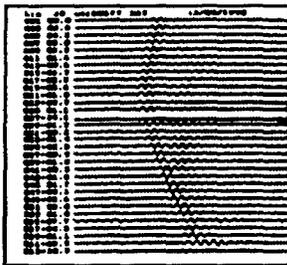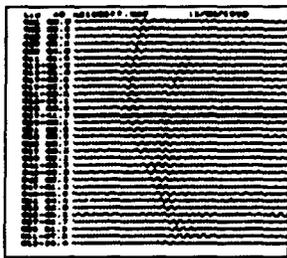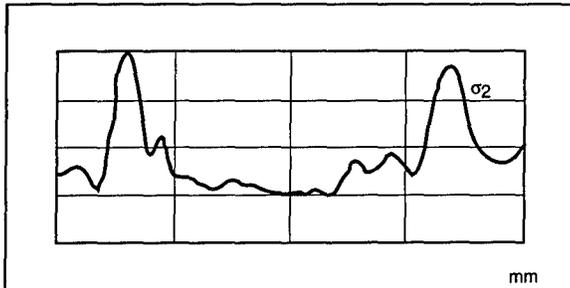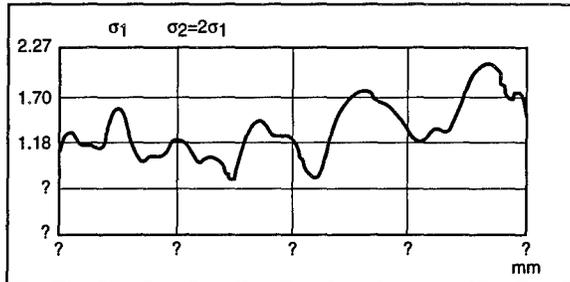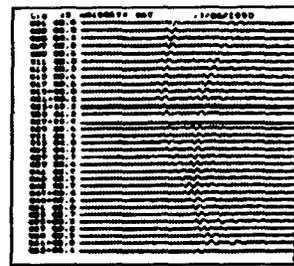
mirror ▦ ■ aberrator

Figure 5-4. Transmit time reversed signal in ottogonal eigenmode.

62

a function of the location along the array from a general iteration of the time reversal process. It is clear that as we iterate the time reversal method, the signal from the wire with the larger cross section rapidly becomes dominant. In Figure 5-4 we have the returns on the array when the signal from the array corresponds to the next eigenmode $V_2(t)$; clearly, here the return is quickly dominated by the return from the second, weaker, scattering wire.

5.2.2 TRACE Caveats

TRACE cannot be perfect at putting a signal back onto its source.

1. Theoretically perfect refocusing of a wave requires fully surrounding the target region with sensors and radiators which sense the outgoing scattered wave without distorting its amplitude or phase. Such a collection of sensors is just not possible. **Nonetheless, this may not be important in practice if the aperture of the sensors and transmitters is large enough to sense scattered waves from the targets of interest in the medium and enough to reradiate back to those sources.** The Prada, Fink experiments demonstrate that much can be accomplished without being 'optimum'.

2. All interesting tissue media have dissipation. In the ultrasound region, this dissipation behaves as $e^{-\beta f}$ in frequency. Dissipation is not time reversal invariant. **Nonetheless, in practice, Fink and colleagues have shown that they can approximately compensate by gain**

corrections at the receiver for this dissipation. This is absolutely not a clear matter yet, so one must go about this carefully.

3. Scattering centers may shadow each other, and thus the interpretation of the eigenfunctions $V_a(t)$ may not be so straightforward.

4. Extended objects appear as the highest 'glint' from their surface, so imaging an extended object may be difficult.

5.2.3   Medical Ultrasound Uses of TRACE

- **Imaging Selected Regions of Tissue:** One can use TRACE to locate and focus acoustic energy into a region where one or more scattering sources are located. It may be necessary to insert contrast agents in the form of bubbles or liquids with sharply different acoustic impedance into the region of interest so one can perform the time reversal focusing.

- **Destruction of Inclusions:** By locating an acoustic scattering object and focusing acoustic energy back onto it, one may be able to destroy that scattering center. Part of the original motivation of Fink's work was to provide methods for destroying gall stones or kidney stones by shattering them acoustically.

- **Potential Tissue Characterization:** If one can characterize tissues by elastic responses at various frequencies or responses to selected temporal waveforms, then utilizing TRACE methods for accelerometer arrays placed on the body, one may be able to focus elastic energy to a

region and characterize the tissues there by the elastic returns. Elastic motions, absent dissipation, are also time reversible. This is a JASON conjecture, and it is neither tested nor proven.

6 TWO-DIMENSIONAL ULTRASOUND AR-RAYS

6.1 Introduction

Medical ultrasound imaging instruments have undergone a long period of development since the invention of ultrasound imaging over thirty years ago, and in many respects the technology is mature. The instruments are highly standardized and they play established roles in medical diagnosis. Even research on new ultrasound technology often uses commercial ultrasound arrays and signal analysis products. Current medical ultrasound systems are generally based on one-dimensional transducer arrays made from piezoelectric elements. These instruments are highly evolved and quite sophisticated, for example phased array beam steering and digital signal processing are commonly used. However, they do not fully benefit from rapid advances in processing technology and integrated electronics, which have revolutionized the semiconductor industry and created the new field of microelectromechanical systems. This new technology changes the ground rules for ultrasound design.

Two-dimensional ultrasound transducer arrays can improve the image quality of conventional medical systems as well as enable new types of ultrasonic imaging, as described elsewhere in this report. The advantages of two-dimensional arrays for imaging have been recognized for some time, but they are impractical using current ultrasound technology. As discussed be-

low, analog-to-digital conversion, high data rates, and even the large number of signal wires pose formidable barriers. In this section, we describe how advanced technology can be used to overcome these barriers and design two-dimensional arrays with integrated readout electronics, and we identify critical aspects of the system that are technically most difficult. To understand the formidable challenges in constructing a two-dimensional ultrasound array, we first consider current practice.

Medical ultrasound technology is based on one-dimensional transducer arrays constructed from piezoelectric elements which act both as transmitters and receivers. A typical array contains about 100 elements of size roughly 0.5×10 mm^2. The lateral dimension of each element is made comparable to the ultrasound wavelength λ for a wide radiation pattern along the scan direction, while the vertical dimension is made much larger in order to narrow the beam in the vertical direction. A cylindrical lens is generally used to focus the beam in the vertical direction to image a two-dimensional slice of the patient ~ 1 cm thick. The one-dimensional array can be constructed by first attaching a slab of piezoelectric ceramic to acoustically dead backing material, then using a diamond saw to separate the elements. Acoustic crosstalk between elements is a serious issue, because the same elements transmit a powerful pulse and receive the weak return signal shortly later. Because the piezoelectric elements are generally hard materials with high velocity of sound, their acoustic impedance is not well matched to the patient, creating reflections and limiting efficiency. For the same reasons, ceramic elements are commonly underdamped, and have acoustic resonances that must be accounted for in system design, usually by driving on resonance to produce a

ringing pulse.

The electronic design of medical ultrasonic systems is particularly challenging. In current systems, each element is attached to a separate shielded wire that passes from the handset to a console that contains the electronics for pulse generation, reception, and image formation. For arrays with many elements, wiring the array can be difficult, and the handset cable becomes quite bulky. The electronics for pulse generation and reception have quite different requirements. Piezoelectric elements can generate powerful ultrasound pulses, but require large excitation voltages > 100V, which in turn require special high voltage electronics. The signal received from the patients is far less, due to the $1/R^4$ loss in scattered intensity with distance R and to the frequency dependent exponential attenuation of ultrasound in the patient at roughly 1 dB/cm-MHz. Returns from the skin at short times can be ~1V, while returns from deep inside the patient fall to levels ~ 1 μV. This large dynamic range exceeds the capability of most analog-to-digital converters and requires the use of a swept gain amplifier or logarithmic amplifier to avoid overload at short times yet provide adequate sensitivity at low levels for imaging. For digital systems, the analog-to-digital converters must have good amplitude resolution and high bandwidth. Good amplitude resolution ~12 bits is required in order obtain good beam patterns from the phased array with high side lobe rejection ratios. High bandwidth, roughly ten times the ultrasound frequency, is necessary for provide good phase accuracy and depth resolution, for example 40 MHz bandwidth for 4 MHz ultrasound frequency. In order to be economically competitive, all of these criteria must be met at low cost, currently ~ \$100/channel for a 100-channel system.

69

Given the design criteria for ultrasound arrays one can understand why two-dimensional arrays have been considered impractical. For example, a two-dimensional array with 100×100 elements made using current ultrasound technology would require hand wiring 10,000 elements to 10,000 separate cables leading from the handset to the electronics console. At \$100/channel, the total cost of the electronics for this system would be $\sim$\$1,000,000. The power consumption of the electronics would be very high, and the computational requirements for image formation would be formidable.

6.2 Two-dimensional Ultrasound Arrays

Rapid advances in semiconductor processing technology, driven by the need for fast low-cost microcomputers, have led to an exponential growth in number of transistors per chip with time, known as Moore's law. Industry projections (the Semiconductor Industry Association "Roadmap") predict that exponential growth will continue at the present rate over the next fifteen years. According to these projections, one chip will hold processors giving a total of 10^{12} op/sec and 2 GBytes of memory. Reduction in feature size can also have important benefits for ultrasound systems: increased computational speed, reduced power consumption, and reduced cost. Packaging technology has advanced in parallel with integrated circuit technology. Highly sophisticated multilayer circuit boards can be used to wire together many separate integrated circuits in compact packages including shielding and heat sinking. Integrated circuits made from different semiconductors can be bonded together in a small number of steps. Photonics can be used

to transmit digital signals with wide bandwidths > 1 GHz over long distances with little cross talk or attenuation. Applied to ultrasound technology, these advances could overcome the seemingly formidable barriers to the fabrication of two-dimensional imaging arrays.

Figure 6-1 illustrates how a two-dimensional ultrasound transducer array could be assembled using advanced packaging technology. This arrangement is motivated by the design of the HIDAD infrared imaging bolometer array manufactured by Texas Instruments. The HIDAD array consists of $\sim$ 240$\times$350 separate Barium Strontium Titanate (BST) pixels, each $50 \times 50 \, \mu m^2$, bonded to a separately fabricated Si integrated circuit containing much of the readout electronics. The pyroelectric ceramic elements in the HIDAD array have similar physical characteristics to piezoelectric ceramic elements used in ultrasound arrays, and are fabricated in a similar manner by dicing a slab of BST ceramic supported by backing material. Unlike most ultrasound arrays, the HIDAD pixels are bonded in one process to the Si readout electronics. Similar techniques have been developed to attach infrared detector arrays made from InSb and other materials to Si integrated circuits.

Exponential reductions in device size and power consumption, will permit much of the transmit and receive electronics for a two-dimensional ultrasound array to be mounted in the handset. The large size of an ultrasound array and the need for separate integrated circuits for transmit and receive dictate the use of a multilayer circuit board in place of a single Si integrated circuit. The technology of multilayer boards has become quite sophisticated: many surface mounted integrated circuits can be connected together via seven

PZT elements

acoustically damped
backing

multilayer circuit board
with electronics

10cm x 10cm
100 x 100 elements
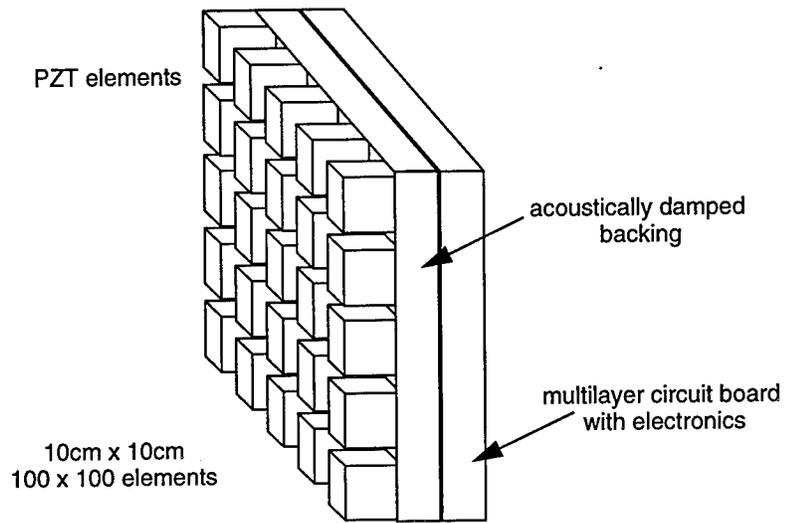
Figure 6-1. Schematic diagram of two-dimensional ultrasound array.

or more wiring layers in a compact package with heat sinking. The chip set for an ultrasound array might include the following: a pulse generator, an analog router, a preamplifier and analog-to-digital converter (ADC) chip, a digital signal processor, and memory. The use of a multilayer board permit wiring of the array and integrated circuits in a few steps, greatly reducing cost, and eliminating problems associated with transmission of weak analog signals from the handset to a separate console.

It is useful to consider the straw man concept of an "ultimate" ultrasound system which consists of a two dimensional array equipped with a complete set of transmit and receive electronics for each pixel. With this ultimate system, the entire time-dependent return signal, and thus the ultrasound image, could be recorded following a single transmitted pulse. Such a system would provide fast time-resolved ultrasound images at high frame rates >1 kHz. As discussed below, the capabilities of the "ultimate" system far exceed the requirements of most medical imaging applications. The ultimate system is interesting nonetheless, because it identifies the envelope of performance for two dimensional arrays and associated design requirements.

A standard ultrasound pulse is formed by applying the same waveform to all elements of the phased array at different times to accomplish beam steering and focus. One can also imagine more sophisticated schemes in which several beams are transmitted at once, for example. Highly sophisticated integrated circuit pulse generators have been developed for current ultrasound systems. The problems posed by the transmit electronics for the "ultimate" array are associated with the high voltages and the high powers

required to excite piezoelectric elements. Because voltages >100 V are required, separate chips made using a high voltage process must be used for the pulse amplifier. A router chip, also made using a high voltage process, can be used to switch the array elements between the pulse generator and the receive electronics.

The total power in the transmitted pulse is potentially quite large and can present a barrier to locating the transmit electronics in the handset. Current regulations permit the use of ultrasonic powers up to $P_{max}/A = 740\,mW/cm^2$; above this level local heating of tissue becomes unacceptable. For current one-dimensional arrays with areas of a few cm^2, the power $P_{max} \sim 4\,W$ is moderate. However for a large two-dimensional array, such as Figure 6-1, application of the maximum statutory power would give $P_{max} \sim 75\,W$, probably too high for safety. Limits on ultrasonic power should be re-examined to account for the characteristics of two-dimensional arrays. Because they can achieve a much sharper three-dimensional focus than one-dimensional arrays, and because they have a much larger receive area, two-dimensional arrays may actually require less total pulse power in order achieve the same signal-to-noise ratio per pulse in a single volume element (voxel) of the image. The time-average total power is then proportional to the number of voxels in the image and the frame rate. If the system is used to record two dimensional images at modest frame rates, the total power could be comparable or less than current systems. However, if three-dimensional images are required at high frame rates, higher power will be required. A careful analysis of imaging properties of two-dimensional arrays and signal-to-noise should be done before reaching conclusions on this issue.

The transmit electronics for two-dimensional arrays with powers comparable to those of current systems could be mounted on the multilayer circuit board as illustrated in Figure 6-1.

Figure 6-2 illustrates the receive electronics for one element of an ultrasound array. The "ultimate" two-dimensional array would contain a copy of the receive electronics for every element. The analog front end consisting of the preamp and analog-to-digital converter (ADC) poses the most difficult challenge for the receive electronics, because it must simultaneously possess high dynamic range ($1\,\mu$V to 1 V), high resolution (> 10 bits), high speed (~ 40 MHz), and low power consumption. The desired dynamic range of 120 dB or 20 bits is too large to be handled by the ADC alone, and requires a swept gain or logarithmic preamplifier. A novel approach to achieving high dynamic range with moderate resolution is the floating-point analog-to-digital converter described in detail below. Conventional fixed-point ADC's with moderate resolution (12 bits) and high sampling rates (40 MHz) are currently available, but typically require powers > 0.1 W. With one converter for each element, the "ultimate" array of 10^4 elements demands lower power consumption as well as a high degree of integration. A separate section of this report describes how the reduction in feature size in advanced integrated circuits permits the design of fast analog-to-digital converters with very low power consumption. Using estimates given in that section for a $0.5\,\mu$m process, we find that a 12-bit, 40 MHz analog-to-digital converter could be designed with power consumption ~ 4 mW. For the "ultimate" system with 10^4 ADC's the total power required ~ 40 W is not as unreasonable as one might have first guessed. The power consumption could be reduced

preamp

analog to digital
converter

memory

processor

12 bit log
40 MHz
4 mW

10k samples/pulse
15kB/element
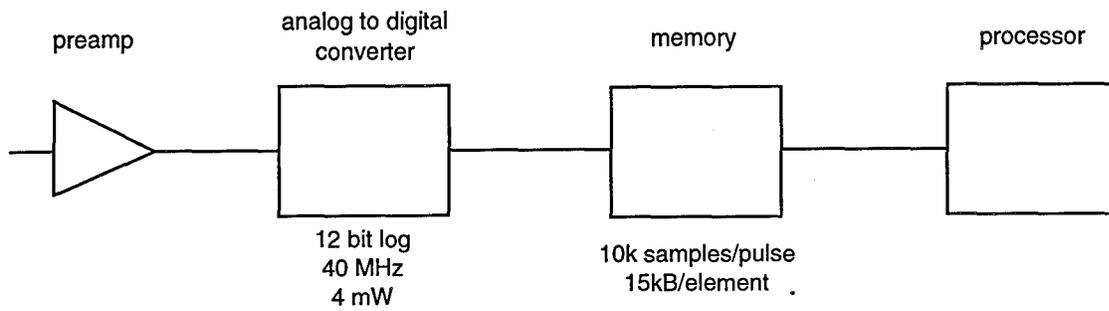
Figure 6-2. Block diagram of the receive electronics for one pixel of the array.

further by reducing the resolution and sample rate, but reduction of the number of ADC's via multiplexing is the best approach for most applications, as described below.

The data rates generated by a two-dimensional ultrasound array can be quite large, and require careful consideration. Following the transmitted pulse, each element of the array receives the return signal for a time $\sim$200 μsec corresponding to a depth $\sim$15 cm into the patient. If the entire transient is digitized the corresponding data rate during reception is (12 bits)(40 MHz) $\sim$ 0.5 Gbit/sec for each element and $\sim$5 Tbit/sec for the entire array. This data rate is too large to transmit in real time from the handset, or even to write to memory in the handset. Because far more data is contained in the ultrasound returns than in a two dimensional image, one can achieve a large reduction in the transmitted data rate by storing each transient and forming the image in the handset. The memory required to store each transient for the example above is 12 kB/element or 120 MB for the entire array. This amount of memory is large, but not unreasonable, and could be mounted on the multilayer backing board in the future. A more serious problem is presented by memory bandwidth, which severely limits the amount of data that can be stored following each pulse. The rate at which one can write to memory is limited to $\sim$100 MB/sec per chip, roughly independent of chip size, and is not expected to increase greatly in the near future. If one uses fifteen 64 Mbit chips to make up 120 MB of memory, the total bandwidth is only $\sim$12 Gbit/sec, far less than the 5 Tbit/sec required by the "ultimate" system. Multiplexing in some form must be used to piece together an image over many pulses. Once the image is formed, it can easily be stored and transmitted

from the handset. A 100×100 pixel image with 12 bits of intensity resolution requires only 15 kB of memory, and the average data rate at the video frame rates is ~ 0.5 MB/sec, easily achievable using a single coaxial cable or fiber optic link.

The processing necessary to form an image from a two-dimensional array is relatively straightforward, but can be formidable for large two-dimensional arrays. For each pixel or voxel in the image, the received signals from each element of the array must be added with the correct delays to steer and focus the beam. The total number of additions N_{op} to form the image is proportional to the number of elements N_{el} and to the number of pixels N_{pix}. For a two-dimensional image with $N_{pix} = N_{el}$ pixels, the total per frame is $N_{op} \sim N_{el}^2$, and for a three dimensional image with $N_{vox} = N_{el}^{3/2}$ the total is $N_{op} \sim N_{el}^{5/2}$. Our "ultimate" system with $N_{el} = 10^4$ elements requires large numbers of operations per frame: $N_{op} \sim 10^8$ for a two dimensional image and $N_{op} \sim 10^{10}$ for a three-dimensional image. To estimate the influence of processing speed on frame rate we note that fast digital signal processors currently achieve speeds ~ 10 Gops/sec; the performance is projected to increase by a factor of 100 over the next 15 years to ~ 1 Tops/sec. Thus the time required to form a two-dimensional image in the example above using one processor chip is currently ~ 0.1 sec, for a three dimensional image ~ 10 sec are required. These times are reasonable, and will improve with increased processor speed in the future.

The "ultimate" system discussed above helps identify critical requirements for two dimensional ultrasound arrays — the need for low-power high-

speed analog-to-digital converters with wide dynamic range, the high data rates generated during pulse reception, and the need for processing power. Surprisingly, we find that a hand-held two-dimensional array with many of the features of the "ultimate" system probably could be built in the not too distant future. The most serious limitation is currently memory bandwidth, which limits the amount of data stored after each pulse. However, the "ultimate" system is wasteful of electronic resources and is probably not the best way to design a two-dimensional imaging ultrasound array. Because the data rate is limited by memory bandwidth and the frame rate is limited by processing speed, multiplexing can be used to reduce the component count and data acquisition rates without loss of capability.

Figure 6-3 illustrates a promising concept — a confocal two-dimensional imaging ultrasound array — which has important advantages for image quality and could be constructed in the near future. In this concept, the aperture of the array is made sufficiently large (10×10 cm^2) to focus each transmitted pulse into a small voxel inside the patient of volume $\sim \lambda^3$, where λ is the ultrasound wavelength. The beam pattern for the return signal is similarly focussed on the same voxel, so that the return from each pulse gives the image from one spot inside the patient. The full image is then constructed by scanning the focal spot across a two-dimensional sheet inside the patient, at one pulse per voxel. The advantages of confocal imaging are insensitivity to diffuse scattering, because the signal from the focal voxel is heavily weighted, and tolerance of aberrations, because both the transmitted and received signal follow the same path through the medium. Confocal imaging was developed for optical microscopy and is used as a powerful tool to

79
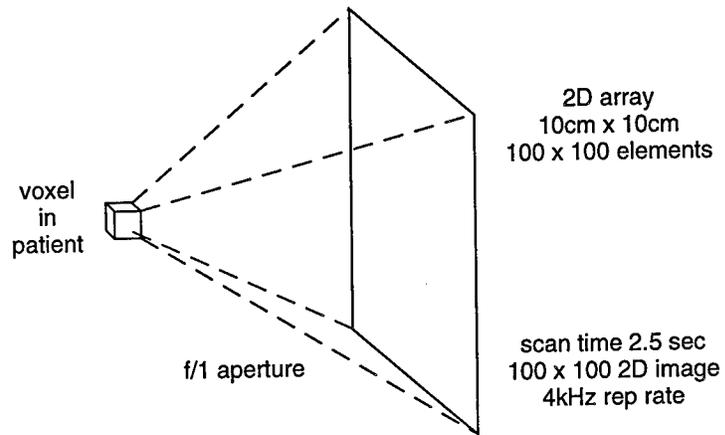
Figure 6-3. Schematic diagram of confocal two-dimensional ultrasound array.

voxel
in
patient

2D array
10cm x 10cm
100 x 100 elements

f/1 aperture

scan time 2.5 sec
100 x 100 2D image
4kHz rep rate

provide sharp images from the interior of strongly scattering media such a biological samples, for which conventional microscopy gives poor results. Focussing of both the transmitted and received beams is currently used with one-dimensional ultrasound arrays to improve intensity, but the focal spot is not small enough for good imaging, due to the small numerical aperture, particularly in the vertical direction. Confocal imaging has been used for special ultrasound applications with very good results. The primary disadvantage of all confocal systems is the time required to form the scanned image. For medical ultrasound the maximum pulse rate is limited by the speed of sound to < 5 kHz, so that ~ 2 sec are required to form a 100×100 pixel image.

Because a confocal ultrasound system samples only one voxel per pulse, the data rate, storage, and computational requirements are far less than those for the "ultimate" system discussed above. Figure 6-4 illustrates one example of how multiplexing can be used to reduce the component count and requirements for the receive electronics of a confocal ultrasound array. Because the received signal is needed only at a single time following the pulse, a track-and-hold amplifier can be used for each element to record the analog signal, which is digitized later by a small number of multiplexed analog-to-digital converters, and summed to obtain the intensity at the focal voxel. For example, as illustrated in Figure 6-4, one analog-to-digital converter can readout each row of a 100×100 array, reducing the number of ADC's by the multiplexing ratio 100:1. Because the delay time resolution is determined by the track-and-hold amplifier, the digitizing rate of the analog-to-digital converter can be relatively slow ~ 400 KHz, just fast enough to readout the elements in each row following each pulse. The reduced number of converters

81

track/hold   multiplexer

analog to digital
converter   memory

12 bit log   12 bits/element
400 kHz

100:1
100   120 kB memory
10,000   100   100
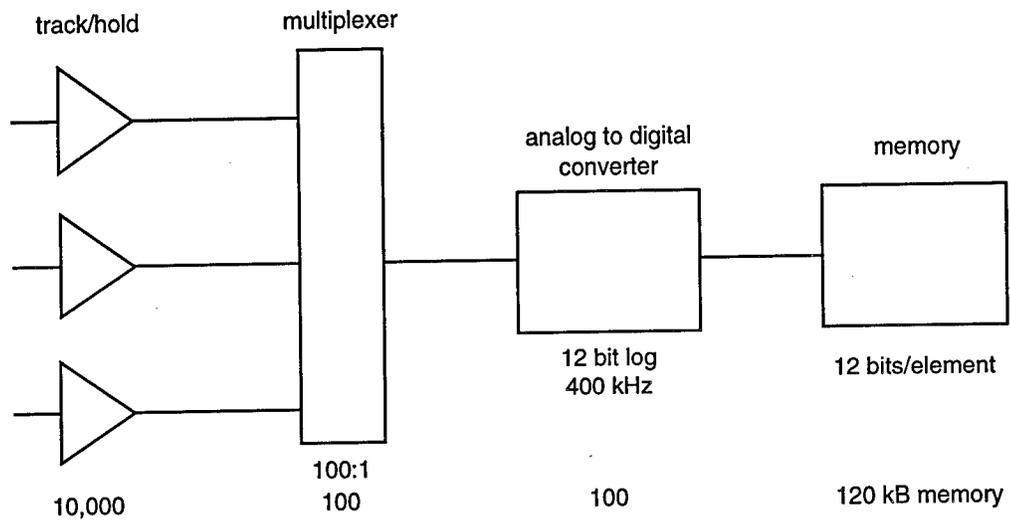
Figure 6-4. Block diagram of the electronics for confocal ultrasound array.

and their reduced speed greatly eases constraints power consumption, so the system can be built with current technology. Similar configurations of multiplexed analog-to-digital converters have been used to make low-cost visible imaging arrays fabricated with CMOS technology.

The field of micro electromechanical systems (MEMS) has developed rapidly in the last decade as an offshoot of integrated circuit processing technology. In addition to micromotors and smart sensors, it is now possible to design entire systems incorporating mechanical and electronic elements on one chip. An overview of recent developments in this area is given in the 1995 JASON report "Micro Electro-Mechanical Systems". The field of medical ultrasound imaging can profitably make use of developments in the MEMS area to design and fabricate new types sensor arrays.

One possible application for MEMS technology in ultrasound is the integrated capacitive sensor illustrated in Figure 6-5. As shown, a capacitor is formed by two plates: a flexible silicon nitride diaphragm coated with a metal film and a fixed metal film plate attached to the substrate. Small displacements register as changes in capacitance between the plates which can be measured via a charge amplifier. Capacitive pressure sensing is a well-established technique favored for its high sensitivity and for the simplicity of the sensing element; a common application is in condenser microphones. Fabrication of capacitive pressure sensors using integrated circuit technology for micro-electromechanical systems has been accomplished using a number of different techniques. Figure 6-5 illustrates one approach: a window containing a flexible free-standing silicon nitride membrane is fabricated in a Si
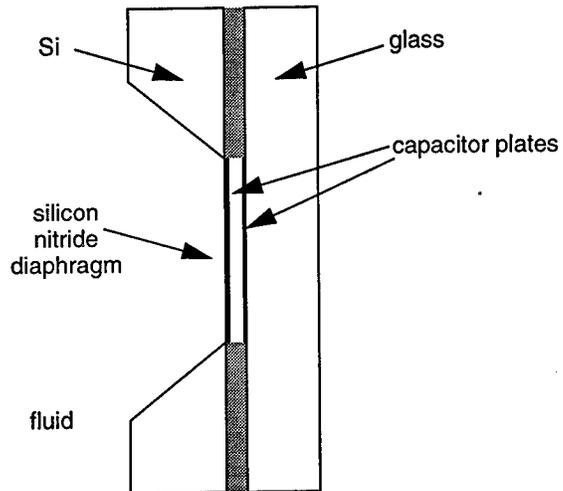
Figure 6-5. Schematic diagram of capacitive ultrasound sensor made using MEMS technology.

wafer using an anisotropic etch on the back side of the wafer. When the Si chip is bonded to a separate glass substrate via a spacing layer, the capacitive sensor is formed. Because the gap between capacitor plates can be made quite small, the sensor can have excellent sensitivity. The frequency response of freestanding membranes is limited by mechanical "drumhead" resonances of the membrane, and is probably inadequate for most ultrasound applications. In order to improve the ultrasonic response, and to obtain good acoustic impedance matching, the diaphragm can be immersed in fluid. If sufficiently light and flexible, the diaphragm accurately follows displacements of the fluid as desired, and its harmonic motion is heavily overdamped. As receivers, capacitive sensors generally have better sensitivity than piezoelectric elements, and when immersed, could give excellent acoustic impedance matching and wide band frequency response for ultrasonic signals without unwanted ringing or phase shifts. Small numbers of capacitive pressure sensors have been fabricated using current MEMS technology. The extension of these techniques to large arrays of capacitive ultrasound transducers appears to be relatively straightforward. A drawback of capacitive ultrasound sensors is the need for a separate piezoelectric array to generate the transmitted pulse. For some special applications such as bistatic or multistatic ultrasound systems, this is not a problem.

It is interesting to note that capacitive sensors of the type shown in Figure 6-5 can be used as ultrasound sources analogous to electrostatic loudspeakers, although the maximum power generated appears to be insufficient for medical ultrasound. The electrostatic energy of the capacitive sensor is $U = (1/2)CV^2$ where V is the applied voltage and $C = \epsilon A/d$ is the capaci-

tance with A the area, d the plate separation, and ϵ the dielectric constant. The pressure created by an applied voltage is $p = -U/Ad$. Because the plate spacing can be quite small, $d \sim 10 \,\mu\text{m}$, modest voltages applied across the capacitor create large electric fields comparable to those used in electrostatic loudspeakers. The force of the applied electric field on a charged membrane immersed in fluid is directly transferred to the fluid if the membrane is sufficiently light and flexible. For water the high dielectric constant $\epsilon = 80$ at low frequencies increases the capacitance and thus the pressure. Using these expressions for the example above, we find that a modest applied voltage $V = 10$ V produces a sound pressure of 5 N/m^2 in air and 400 N/m^2 in water; the latter corresponds to a sound intensity ~ 0.1 W/m^2 in water. These sound levels are large enough to be interesting and perhaps useful for special applications, but are much lower than those generated by piezoelectric transducers.

6.3 Floating Point Analog to Digital Conversion for Ultrasound Applications

When converting analog signals, such as those from acoustic transducers in ultrasound systems, which have a large dynamic range $\sim 10^6$ but do not require comparable precision, a floating point analog-to-digital converter can be used. A floating point ADC preserves the precision of the signal without needing a higher resolution converter or introducing the uncertainty associated with swept gain amplifiers. This technique is used at low precision in companding A-law and μ-law codecs to represent analog signals in digital

86

telephone systems.

A floating point analog-to-digital converter accepts an analog signal and outputs a floating-point number. The output has three components: sign s, fraction f, and exponent n. The value represented by a particular s, f, and n is given by the mapping function

$$M(s, f, n) = -1^s 2^n K f$$

where K is a scale factor, and f and n are binary numbers. To represent ultrasound data, for example, we could use a 15-bit number with a 10-bit fraction and a 4-bit exponent. This gives an unscaled range from 0 to $\pm 33,521,664$ (1023×215) with a resolution at value N of $\max(1, 10^{-3}N)$. With an appropriate scaling factor, the dynamic range is $30\,\text{nV}$ to $1\,\text{V}$ with all signals over $30\,\mu\text{V}$ having a constant precision of 10^{-3}.

An analog signal can be directly converted to an N-bit floating point number in N successive approximation steps using the circuit shown in Figure 6-6. The logic follows the following sequence:

1. The fraction f is initialized to have a leading 1 and the remaining bits set to zero.

2. For the first comparison step the input signal, scaled by the exponent, is compared to zero. If negative the sign bit is set and the signal is multiplied by -1 for the remaining steps.

3. For each bit n_i of the exponent n from left to right, the bit n_i is cleared and the input signal scaled by $2^{-n}K$ is compared to the fraction f
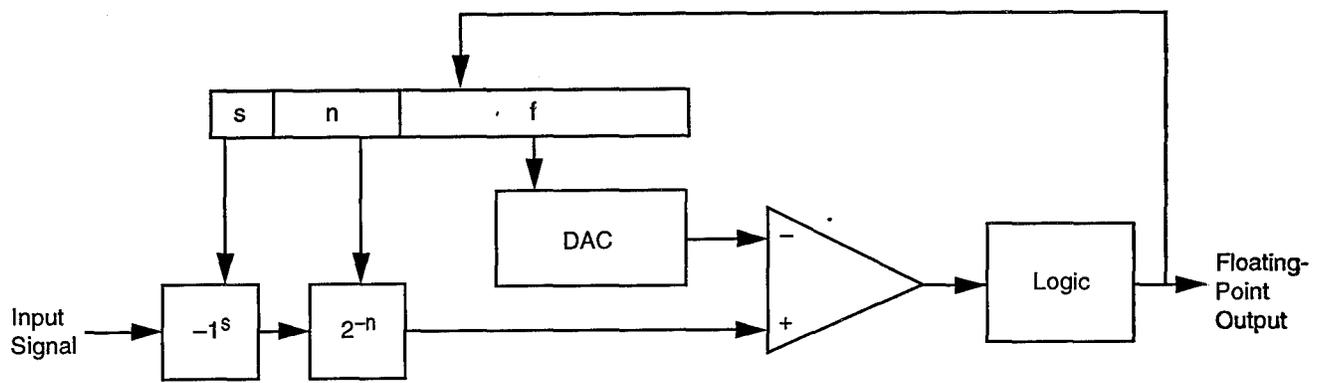
Figure 6-6. Block diagram of floating point analog-to-digital converter.

which was set at half range in step 1. If the signal is larger than half range, n_i is set. If the signal is smaller than half range, n_i remains cleared. In either case we advance to bit n_{i+1} for the next cycle.

4. For each bit f_i of the fraction f, set f_i and compare the input signal scaled by $2^{-n}K$ to f. If the scaled signal is greater than f, f_i remains set; otherwise f_i is cleared. In either case, advance to bit f_{i+1} for the next cycle.

After 15 cycles, this procedure computes the values of s, n, and f that map to the value closest to the input signal.

A floating point analog-to-digital converter is much easier to construct and operates faster than a linear converter with the same dynamic range. A linear ADC with the same dynamic range as our 15-bit floating-point example would require 25 bits. It is infeasible with existing technology to fabricate a digital-to-analog converter with sufficient linearity to build such an ADC. Even if it were possible, such as converter would take 25 successive approximation cycles, and some cycles would need greater time for signals to settle to very high precision. The floating-point converter will need to be calibrated to correct for imperfections in its 2^{-n} stage. This is much easier than calibrating a linear converter, as we need only store 15 correction factors (one for each non-zero exponent) rather than 2^{25}.

Compared to a swept-gain amplifier, the floating-point ADC has two advantages. First, all signals acquired are of the same known scale. This simplifies combining signals taken at different times, for example during beam

89

forming. Second, the floating-point ADC applies its large dynamic range to all input samples. Thus small samples taken near zero crossings of the signal during the early part of an echo when the envelope of the signal is large and the gain small will be digitized with full precision. With swept gain and a linear ADC with the same number of bits, such signals would be digitized with much lower precision.

6.4   Conclusions

Medical ultrasound imaging systems are highly sophisticated in many respects. They have evolved since their invention over thirty years ago, and certain aspects of their design reach back to that time. In this section we have attempted to demonstrate that rapid advances in integrated electronics have created opportunities for the implementation of fully two-dimensional ultrasound imaging systems. Two dimensional ultrasound arrays should permit sharper two-dimensional images of tissue by focussing in the vertical direction, and they can make fully three dimensional images. With integrated sensors and electronics two-dimensional arrays may become cost effective adjuncts or replacements for magnetic resonance imaging and other three dimensional imaging technologies.

7 LOW-POWER A/D CONVERSION

7.1 Overview

We have already pointed out the importance of low-power analog-to-digital (A/D) conversion for large ultrasound arrays. This report analyzes the power dissipation of a straightforward A/D converter.

7.2 Block Diagram

Figure 7-1 shows a block diagram of a typical A/D converter. Each sample interval an analog input signal is placed on the positive input of a comparator. The "logic" and "D/A" blocks then generates a series of voltages to which the input is compared. The output is generated as a result of these comparisons.

Different styles of A/D converters vary the sequence of voltages being compared and the manner in which they are generated. Some popular styles include:

1. Successive Approximation: The logic generates a series of voltages that perform a binary search for the input voltage by repeatedly halving the interval in which the voltage may be contained. This generates an b-bit digital output in b steps with the output of the comparator containing
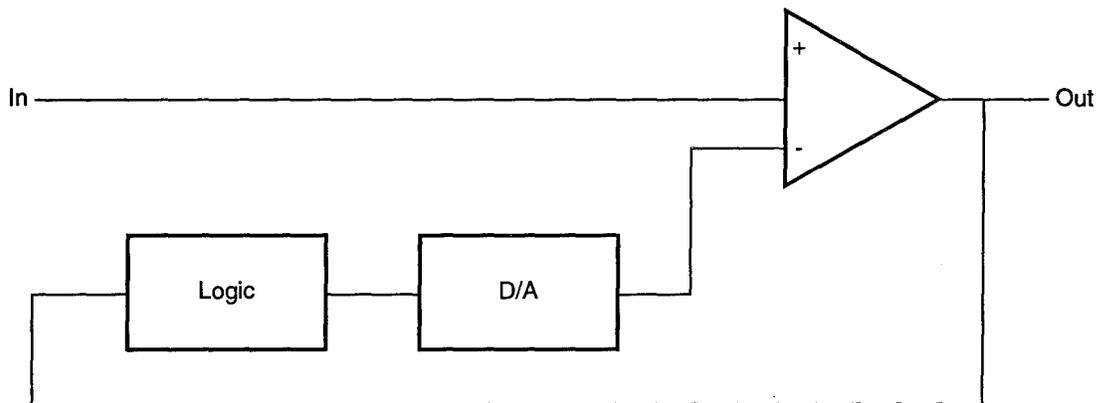
Figure 7-1. A/D Converter Block Diagram.

the bits of the output MSB-first. The binary search can be performed serially in a single stage or as a pipeline of stages, one per bit.

2. Slope or Dual-Slope: The logic generates a "ramp" independent of the comparator output and the point at which the comparator switches indicates the input voltage. The ramp is usually generated by an analog integrator while the time interval is measured by sampling a free-running counter. This method requires 2^b steps to generate an b-bit output.

3. Oversampled: The logic closes a loop that "delta-codes" the input. That is the logic counts up when the output of the comparator is one and down if it is zero. Some converters use delta-sigma rather than straight delta coding. In either case an integrator can be used to generate the voltages eliminated the need for a full D/A. The output stream is decimated to produce an b-bit digital signal at 2^{-b} the original sample rate. These converters are popular in systems where the oversampling and decimation obviate the need for analog anti-aliasing filters with sharp cut-offs.

4. Flash: A flash converter performs all of the operations of a slope converter, but in parallel rather than serially. A resistive or capacitive voltage divider generates 2^b equally-spaced voltages and 2^b comparators compare the input signal to all of these voltages simultaneously. A log-depth logic circuit encodes the output of the comparators into a b-bit signal. Flash converters are used in situations where very low latency is required. For total throughput a successive approximation converter is preferred as b successive approximation converters have the

same throughput as a single flash converter at $b/2^b$ the cost.

5. Hybrid: A hybrid converter is a successive approximation converter that uses an m-bit flash converter at each stage to perform a b-bit conversion in b/m steps. Rather than using a D/A in a feedback loop, the signal is usually recentered and rescaled between each step to perform the 2^m-ary divide and conquer search.

7.3 Power Calculation

Consider the problem of performing a b bit A/D conversion with sample rate f. If a successive approximation converter is used, the energy required for the conversion is

$$P_{sa} = fb(E_c + gE_{sw} + E_{sda})$$

where E_c is the energy required per comparison, E_{sw} is the switching energy of the technology, g gates switch for the logic to prepare for each comparison, and E_{sda} is the D/A conversion energy. Each of these components of power is dealt with in more detail below.

The slope-based and oversampling converters require considerably more power than this because although they have simpler logic and D/A components this advantage is overwhelmed by the fact that they perform 2^b comparisons to convert a b-bit number rather than b.

94

7.3.1 Comparator

The comparator can be realized as a clocked sense-amplifier, as a static differential amplifier, or as an inverter with a switched capacitor input. In the case of the static amplifier, the current bias is set so it has just enough output current to swing its output capacitance in one bit time. A self-biasing circuit can be used to adjust the current source to this minimum current value. The output capacitance includes the self capacitance of the amplifier, a small amount of wiring capacitance, plus a minimum-sized inverter to buffer the signal for distribution to the logic. If transistor sizes are kept small a total capacitance of 50fF is reasonable in an 0.5μm process. Assuming half the bias current goes into the output and a 3.3V supply voltage this gives a comparison energy of

$$E_c = 5 \times 10^{-14}(3.3^2)(2) \approx 1\text{pJ}$$

With the clocked sense amplifier the clock load is increased by about 10fF to drive isolation devices and to gate on the amplifier current source. Also the regenerative feedback slightly increases the self-capacitance of the amplifier, to about 70fF for typical device sizes. Thus a clocked sense-amp would have a slightly higher comparison energy of about 1.6pJ but would have the advantage of not requiring a speed-dependent bias current.

An inverter with a switched input capacitor would have a somewhat larger power dissipation as it requires a DC current (when operated in the middle of its range), current to charge its input capacitor, and clock power to drive the switches.

7.3.2 D/A

The D/A converter can be realized using switched capacitors, with an R-2R ladder, or with a series of progressively-sized transistors. The R-2R approach will not be considered as precise-valued resistors are hard to fabricate on an MOS integrated circuit.

The switched capacitor D/A takes advantage of the subdivision property of the voltage sequence in a successive approximation A/D converter to produce the required voltage sequence by charge sharing between two equally sized capacitors. Initially one capacitor is charged high and the other low to bound the interval. A capacitive voltage divider is then used to find the midpoint of the interval. This midpoint voltage is then placed on one of the two capacitors to define the next interval and the process is repeated.

This approach requires two voltage followers that must have enough bias current to copy voltages accurately in a bit time. With 100fF capacitors, each follower would consume about 2pJ per bit and another 2pJ would be used in charging each capacitor for a total of 8pJ per bit.

The transistor approach, which to my knowledge is original, replaces the negative input of the comparator with a parallel connection of NFETs with progressively increasing sizes. Rather than being connected to an analog voltage, the gates of these transistors are directly controlled by the logic. They are sized so that the comparator will "trip" when the input voltage exceeds the binary value encoded on the transistor gates. The sizes are not

96

simply powers of two, but rather must match the quadratic I-V characteristic of the MOSFET.

The only power consumed by this approach is caused by the increased capacitive load on the output of the logic which switches at most once per cycle. For small b, this load is small but for large b it increases exponentially. A rough expression for the energy required per bit is:

$$E_{sda} = 0.1(2^{b/2})/b\text{pJ}$$

For an 8-bit signal, this is just 0.2pJ per bit.

Alternatively power-of-two sized transistors can be connected to a polysilicon load resistor to generate a voltage that is a linear function of the binary input. This will roughly double the comparison energy.

In either case, capacitance is minimized by using a minimum sized device in the middle of the size range and using devices with minimum L and $W > L$ in the upper half of the range and minimum W and $L > W$ in the lower half of the range.

7.3.3   Logic

The logic required for a serial successive-approximation converter is a register to hold each bit of the current digital value, and ring-counter shift register to select the next bit to update, and a MUX to select the input to each bit of the register. Each register bit toggles exactly once per conversion

cycle as does each ring counter bit. If we count switching each register as four switching events and add two switching events for the associated MUX, the constant g is 10 switching events per bit. With an E_{sw} of 0.1pJ this gives a logic energy of 1pJ per bit. For a pipelined converter the ring counter and multiplexer are not required reducing this power slightly.

7.3.4 Example

For example a $b = 8$-bit converter with a transistor D/A operating at 1 MHz would have a total power dissipation of

$$P_{sa} = 8 \times 10^6(1\text{pJ} + 0.2\text{pJ} + 1\text{pJ}) \approx 20\mu\text{W} .$$

Even if we increase this by a factor of 5 to use the 1.6pJ sense amp, the 8pJ capacitive D/A and to account for overhead, the power is still only 100μW.

7.4 Other Issues

7.4.1 Resolution and Linearity

To operate at very low power, one uses minimum sized devices. These devices can have relatively large parameter mismatch (on the order of 10%) which limits the linearity of the converter. It is more power efficient to correct these linearities digitally via a PROM than it is to increase the component size to eliminate them.

To get adequate resolution in the presence of mismatches, capacitor leakage, and other effects, the converter may have to produce more bits of intermediate result than are required in the final linearized result. The converter must resolve voltage steps that are no more than one LSB apart. Usually adding one additional bit is sufficient to provide this spacing.

7.4.2 Low-Voltage Operation

The analysis above has not considered the possibility of voltage scaling. If the circuit is operated slowly, the supply voltage can be reduced which reduces power quadratically. While very slow circuits can be operated in the subthreshold region, most practical circuits are limited to supply voltages of about 1V to remain comfortably above the device threshold. At 1V power is reduced by a factor of 9 over the numbers calculated above. Low voltage operation does require that the input voltage be scaled to the small power supply.

References

[1] Freiburger, P.D., Sullivan, D.C., LeBlanc, B.H., Smith, S.W. and Trahey, G.E., "Two-dimensional ultrasonic beam distortion in the breast: in vivo measurements and effects," *Ultrasonic Imaging* 14, 398-414 (1992).

[2] Zhu, Q. and Steinberg, D., "Large-transducer measurements of wavefront distortion in the female breast," *Ultrasonic Imaging* 14, 276-299 (1992).

[3] Rose, J.H., Kaufmann, M.R., Wickline, S.A., Hall, C.S. and Miller, J.G., "A proposed microscopic elastic wave theory for ultrasonic backscatter from myocardial tissue" *J. Acoust. Soc. Am.* 97, 656-668 (1995).

[4] Fink, M., "Time reversal of ultrasonic fields: basic principles," *IEEE Trans. Ultrason. Ferroelectr. Freq. Control* 39, 555-566 (1992).

[5] Sarvazyan, A. et al., "Elasticity imaging as a new modality of medical imaging for cancer detection", *Proc. Int. Workshop on Interaction of Ultrasound with Biological Media* (Valenciennes, France), 69-81 (1994).

[6] Cornwall, J.M., Flatté, S.M., et. al., "Biomedical Imaging" JASON Report JSR94-120 (1994).

[7] Hinkelman, L.M., Liu, D.L., Metlay, L.A. and Waag, R.C., "Measurements of ultrasonic pulse arrival time and energy level variations produced by propagation through abdominal wall," *J. Acoust. Soc. Am.* 95, 530-541 (1994).

[8] Krammer, P. and Hassler, D., "Measurement of spatial time-of-flight fluctuations of ultrasound pulses passing through inhomogeneous layers," in *1987 IEEE Ultrasonics Symposium Proceedings"* pp 939-942.

[9] Zhu, Q. and Steinberg, D., "Measurements of ultrasonic pulse arrival time and energy level variations produced by propagation through abdominal wall," *J. Acoust. Soc. Am.* 96, 1-9 (1994).

[10] Trahey, G.E., Freiburger, P.D., Nock, L.F. and Sullivan, D.C., "In vivo measurements of ultrasonic beam distortion in the breast," *Ultrasonic Imaging* 13, 71-90 (1991).

[11] Flatté, S.M., et. al., *Sound transmission through a fluctuating ocean*, (Cambridge University Press, 1979).

[12] Flatté, S.M., "Wave propagation in random media: Contributions from ocean acoustics," *Proc. IEEE* 71, 1267-1294 (1983).

[13] Waag, R.C., "A review of tissue characterization from ultrasonic scattering," *IEEE Trans. Biomed. Eng.* BME-31, 884-893 (1984).

[14] O'Donnell, M. and S W. Flax, "Aberration correction without the need for a beacon signal", *Proc. IEEE Ultrasonics Symposium*, 833-837 (1988).

[15] Nock, L., Trahey, G.E. and Smith, S.W., "Phase aberration correction in medical ultrasound using speckle brightness as a quality factor," *J. Acoust. Soc. Am.* 85 (5), 1819-1833 (1989).

[16] Liu, D.-L. and R.C. Waag, "Correction of ultrasonic wavefront distortion using backpropagation and a reference waveform method for time-shift compensation", *J. Acoust. Soc. Am.* 96, 649-660 (1994).

[17] Krishnan, S., P.-C. Li, and M. O'Donnell, "Adaptive compensation of phase and magnitude aberrations", U. Mich. preprint, 1995.

[18] Mallart, R. and Fink, M., "The van Cittern-Zernike theorem in pulse echo measurements," *J. Acoust. Soc. Am.* 90 (5), 2718-2727 (1990).

[19] McCann, H.A. et al., "Multidimensional ultrasonic imaging for cardiology", *Proc IEEE* 76, 1063-1072 (1988).

[20] Witten, A., J. Tuggle and R.C. Waag, "A practical approach to ultrasonic imaging using diffraction tomography", *J. Acoust. Soc. Am.* 83, 1645-1652 (1988).

[21] Borup, D.T. et al., "Nonperturbative diffraction tomography via Gauss-Newton integration applied to the scattering integral equation", *Ultrason. Imag.* 14, 69-85 (1992).

[22] Devaney, A.J. and M.L. Oristaglio, "Inversion procedure for inverse scattering within the distorted-wave Born approximation", *Phys. Rev. Lett.* 51, 237-240 (1983).

[23] Hopcraft, K.I., and P.R. Smith, "Geometrical properties of backscattered radiation and their relation to inverse scattering", *J. Opt. Soc. Am.* A6, 508-516 (1989).

[24] Zhu, Q. and B.D. Steinberg, "Modeling, measurement and correction of wavefront distortion produced by breast specimens", *Proc. IEEE Ultrasonics Symposium*, 1613-1617 (1994).

[25] Scherzinger, A.L., et. al., "Assessment of ultrasonic computed tomography in symptomatic breast patients by discriminant analysis", *Ultrasound in Med. and Biol.* 15, 1-28 (1989).

[26] Robinson, D.E., C.F. Chen and L.S. Wilson, "Image matching for pulse echo measurement of ultrasonic velocity", *Image Vis. Comp.* 1, 145-151 (1983).

[27] Smith, S.W., G.E. Trahey and O.T. von Ramm, "Phased-array ultrasound imaging through planar tissue layers", *Ultrasound Biol. and Med.* 12, 229-243 (1986).

[28] Greenleaf, J.G. et al., "Multidimensional visualization in echocardiography: An introduction", *Mayo Clinics Proc.* 68, 213-226 (1993).

[29] Ng, Gary C., Stewart S. Worell, Paul D. Freiberger, and Gregg E. Trahey, "A Comparative Evaluation of Several Algorithms for Phase Aberration Correction", *IEEE Transactions on Ultrasonics, Ferroelectrics, and Frequency Control*, 41, 631-643 (1994).

[30] Flax, S. W. and M. O'Donnell, "Phase-Aberration Correction Using Signals from Point Reflectors and Diffuse Scatters: Basic Principles", *IEEE Transactions on Ultrasonics, Ferroelectrics, and Frequency Control*, 35, 758-767 (1988). M. O'Donnell and S. W. Flax, "Phase-Aberration Correction Using Signals from Point Reflectors and Diffuse Scatters: Mea-

surement", *IEEE Transactions on Ultrasonics, Ferroelectrics, and Frequency Control*, **35**, 768-774 (1988).

[31] Nock, L., G. E. Trahey, and S. W. Smith, "Phase Aberration Correction in Medical Ultrasound Using Speckle Brightness as a Quality Factor", *Journal of the Acoustical Society of America* **85**, 1819-1833 (1989).

[32] Fink, Mathias, "Time Reversal of Ultrasonic Fields—Part I: Basic Principles", *IEEE Transactions on Ultrasonics, Ferroelectrics, and Frequency Control*, **39**, 555-566 (1992); Francois Wu, Jean-Louis Thomas, and Mathias Fink, "Time Reversal of Ultrasonic Fields—Part II: Experimental Results", *IEEE Transactions on Ultrasonics, Ferroelectrics, and Frequency Control*, **39**, 567-578 (1992); Didier Cassereau and Mathias Fink, "Time Reversal of Ultrasonic Fields—Part III: Theory of the Closed Time-Reversal Cavity", *IEEE Transactions on Ultrasonics, Ferroelectrics, and Frequency Control*, **39**, 579-592 (1992).

[33] Prada, C., F. Wu, and M. Fink, "The Iterative Time Reversed Mirror: A Solution to Self-Focusing in the Pulse Echo Mode", *Journal of the Acoustical Society of America* **90**, 1119-1129 (1991); C. Prada and M. Fink, "Eigenmodes of the Time Reversal Operator: A Solution to Selective Focusing in Multiple-Target Media", *Wave Motion* **20**, 151-163 (1994); C. Prada, J-L Thomas, and M. Fink, "The Iterative Time Reversal Process: Analysis of the Convergence", *Journal of the Acoustical Society of America* **97**, 62-71 (1995) (1991).

[34] Morse, P. M. and K. U. Ingard, *Theoretical Acoustics*, Princeton University Press, 1968.

DISTRIBUTION LIST

Director of Space and SDI Programs
SAF/AQSC
1060 Air Force Pentagon
Washington, DC 20330-1060

CMDR & Program Executive Officer
U S Army/CSSD-ZA
Strategic Defense Command
PO Box 15280
Arlington, VA 22215-0150

A R P A Library
3701 North Fairfax Drive
Arlington, VA 22209-2308

Dr Henry Abarbanel
1110 Crest Road
Del Mar, CA 92014

Dr Arthur E Bisson
Director
Technology Directorate
Office of Naval Research
Room 407
800 N. Quincy Street
Arlington, VA 20350-1000

Dr Albert Brandenstein
Chief Scientist
Office of Nat'l Drug Control Policy
Executive Office of the President
Washington, DC 20500

Mr. Edward Brown
Assistant Director
ARPA/SISTO
3701 North Fairfax Drive
Arlington, VA 22203

Dr H Lee Buchanan, I I I
Director
ARPA/DSO
3701 North Fairfax Drive
Arlington, VA 22203-1714

Dr Ashton B Carter
Nuclear Security & Counter Proliferation
Office of the Secretary of Defense
The Pentagon, Room 4E821
Washington, DC 20301-2600

Dr Collier
Chief Scientist
U S Army Strategic Defense Command
PO Box 15280
Arlington, VA 22215-0280

Dr John Cornwall
University of California/Los Angeles
Department of Physics
Los Angeles, CA 90024

Dr Ken Cress
Office of Research and Development
Washington, DC 20505

D T I C [2]
Cameron Station
Alexandria, VA 22314

Dr William Dally
University of North Carolina
Department of Computer Science
Sitterson Hall, Campus Box 3175
Chapel Hill, NC 27599

Mr John Darrah
Senior Scientist and Technical Advisor
HQAF SPACOM/CN
Peterson AFB, CO 80914-5001

Dr Victor Demarines, Jr.
President and Chief Exec Officer
The MITRE Corporation
202 Burlington Road
A210
Bedfored, MA 01730-1420

DISTRIBUTION LIST

Dr Stanley Flatte
678 Spring Street
Santa Cruz, CA 95060

Mr Dan Flynn   [5]
OSWR
Washington, DC 20505

Dr Paris Genalis
Deputy Director
OUSD(A&T)/S&TS/NW
The Pentagon, Room 3D1048
Washington, DC 20301

Dr Lawrence K. Gershwin
NIC/NIO/S&T
7E47, OHB
Washington, DC 20505

Mr. Thomas H Handel
Office of Naval Intelligence
The Pentagon, Room 5D660
Washington, DC 20350-2000

Dr Robert G Henderson
Director
JASON Program Office
The MITRE Corporation
7525 Colshire Drive
Mailstop Z561
McLean, VA 22102

Dr William E Howard I I I   [2]
Director of Advanced Concepts &
Systems Design
The Pentagon Room 3E480
Washington, DC 20301-0103

Dr Gerald J Iafrate
U S Army Research Office
PO Box 12211
4330 South Miami Boulevard
Research Triangle NC 27709-2211

J A S O N Library [5]
The MITRE Corporation
Mail Stop W002
7525 Colshire Drive
McLean, VA 22102

Dr Anita Jones
Department of Defense
DOD, DDR&E
The Pentagon, Room 3E1014
Washington, DC 20301

Mr. O' Dean P. Judd
Los Alamos National Laboratory
Mailstop F650
Los Alamos, NM 87545

Dr Bobby R Junker
Office of Naval Research
Code 111
800 North Quincy Street
Arlington, VA 22217

Lt Gen, Howard W. Leaf, (Retired)
Director, Test and Evaluation
HQ USAF/TE
1650 Air Force Pentagon
Washington, DC 20330-1650

Mr. Larry Lynn
Director
ARPA/DIRO
3701 North Fairfax Drive
Arlington, VA 22203-1714

Dr. John Lyons
Director of Corporate Laboratory
US Army Laboratory Command
2800 Powder Mill Road
Adelphi, MD 20783-1145

Col Ed Mahen
ARPA/DIRO
3701 North Fairfax Drive
Arlington, VA 22203-1714

DISTRIBUTION LIST

Superintendent
Code 1424
Attn Documents Librarian
Naval Postgraduate School
Monterey, CA 93943

Ambassador James Sweeney
Chief Science Advisor
USACDA
320 21st Street NW
Washington, DC 20451

Dr George W Ullrich [3]
Deputy Director
Defense Nuclear Agency
6801 Telegraph Road
Alexandria, VA 22310

Dr Walter N Warnick [25]
Deputy Director
Office of Planning &Analysis, ER-5.1
Office of Energy Research
U S Department of Energy
Germantown, MD 2074

Dr Robert Westervelt
Harvard University
Division of Applied Science
Cambridge, MA 02138

Dr Edward C Whitman
Dep Assistant Secretary of the Navy
C3I Electronic Warfare & Space
Department of the Navy
The Pentagon 4D745
Washington, DC 20350-5000

Capt H. A. Williams, U S N
Director Undersea Warfare Space
   & Naval Warfare Sys Cmd
PD80
2451 Crystal Drive
Arlington, VA 22245-5200